Institut und Lehrstuhl für Radiochemie

Technische Universität München

RCM 072008

Wechselwirkungen von Actiniden mit Anorgano-Huminkolloiden

A.N. Priemyshev, M.A. Kim, D.C. Breban*, A. Türler
in collaboration with
P.J. Panak*, J.I. Yun*, J.I. Kim*

Abschlußbericht**
30.06.08

*) Institut für Nukleare Entsorgung, Forschungszentrum Karlsruhe, 76021 Karlsruhe

**) Das diesem Bericht zugrunde liegende Vorhaben wurde mit Mitteln des Bundesministeriums für Wirtschaft und Technologie (BMWi) unter dem Förderkennzeichen 02 E 10035 gefördert. Die Verantwortung für den Inhalt dieser Veröffentlichung liegt bei den Autoren.

Contents

Page

SUMMARY **4**

1 INTRODUCTION **7**

2 EXPERIMENTAL **9**

2.1 PREPARATION OF INACTIVE AND RADIOACTIVE STOCK SOLUTIONS 9
2.2 MOTHER SOLUTIONS FOR ACTINIDE/COLLOIDS INTERACTION 12
2.3 ACTIVITY PARTITION IN SOLUTION, COLLOIDS AND PRECIPITATE 14
2.4 COLORIMETRIC QUANTIFICATION OF SI AND AL 18

3 RESULTS AND DISCUSSION **19**

3.1 HUMIC ACID (HA) AS COLLOIDS: INFLUENCING PARAMETERS 19
3.2 STABILITY OF HUMIC COLLOID-BORNE ACTINIDES 25
3.3 HYDROXYALUMINOSILICATE (HAS) AS COLLOIDS 30
3.4 STABILITY OF HAS COLLOIDS AND COLLOID-BORNE ACTINIDES 33
3.5 COMPLEXATION OF AL(III) AND ACTINIDE(III)/(IV)/(VI) WITH SILICIC AND HUMIC ACIDS 47
3.6 STABILITY AND AVERAGE PARTICLE SIZE OF HAS - HUMIC COLLOIDS 57

4 CONCLUSION **59**

5 APPENDIX A **61**

6 APPENDIX B **68**

7 REFERENCES **69**

8 PUBLICATIONS, REPORTS AND CONFERENCES **71**

ACKNOWLEDGEMENTS **74**

Summary

The present report is a continuation of our study [1, 2] on the generation and characterization of actinide pseudocolloids, in particular, the influence of humic acid (HA) on the formation of hydroxyaluminosilicate (HAS) colloid borne actinides. The following investigation is focused firstly on the humic acid itself as far its colloidal properties are concerned, then on the interaction of humic acid Gohy-573 (HA) with Ca(II), Al(III), Eu(III), Am(III) and Th(IV) ions and finally on the influence of HA on the dissolution kinetic of HAS colloids, as parts of the ultimate objective to predict the distribution and mobility of radionuclides in the environment.

In the first part of the work, the influence of pH, temperature and the concentration of the humic acid itself on its partition between the precipitate, colloids and solution is investigated. The effect of Ca, Al, Eu and Th ions on the destabilization of humic colloids is also examined. It is found that Eu is the most effective coagulant among other metal ions. The obtained results indicate that for any given pH, colloid HA possess to hold tri-, tetra and hexavalent cations in higher amounts than weakly coordinated divalent calcium ions if the metal concentration does not exceed the proton exchange capacity of HA. The stability of colloidal ^{14}C-radiolabelled humic substances is tested by filtration and ultrafiltration combined with liquid scintillation counting and UV/Vis spectroscopy. In one sample series the HA concentration is kept constant at 6 mg/l and the pH is varied from 4 to 9. A slightly elevated precipitate fraction is observed at pH<5.5 due to the beginning of the protonation of the HA functional groups leading to aggregation. In the neutral pH region, the fraction regarded as humic colloids after a sample conditioning time of 35 days is found to reach approximately 75 - 80%. At longer conditioning time, however, slightly elevated precipitate and ionic fractions are observed. In another sample series the pH is kept constant at 6.6 in 0.01 M MOPS buffer and the HA concentration is gradually increased from 0.6 to 10 mg/l. A variation of the HA concentration has only negligible effects on the partition of HA. The impact of temperature on the stability of the HA is studied with solutions of 6 mg/l HA at pH 7.8 (10^{-2} M MOPS buffer). Solutions are kept in water bath for 4 days storage at different temperatures up to 90^{o}C. The difference between UV/Vis absorption of HA solution stored at room temperature and the absorption of the HA solution stored at 90^{o}C is small but well reproducible. At 90^{o}C, the spectrum shows a slight change with an increase towards shorter wavelengths. This indicates that aggregation

of HA occurs which induces the increase in the UV absorbing properties of HA. The fractionation tests demonstrate that HA colloids are dissolved and precipitated at the same time. The result shows that rearrangement of HA takes place already at 40^{o}C. With increasing temperature the expected increase in conversion velocity is found.

In the second part of the work, the stability of Th(IV) and Am(III) humate complexes are investigated using a competing ligand displacement method. The effects of initial [Th]/[HA] concentration ratio, predissociation equilibration time, and temperature on the rates of complex dissociation are studied. In a separate experiment the competition between Th and Am for generation of humate colloid-borne actinides is investigated. Solutions containing the metal humate complexes are spiked with appropriate amounts of EDTA. The differentiation between colloid-borne metal species and the metal – EDTA complexes formed as a function of time is carried out by sequential filtration, first at 450 nm pore size (Sartorius) and then the resulting filtrate at about 1.5 nm nominal pore size (Centricon YM-10, Millipore). The dissociation kinetics and the apparent equilibrium of the exchange reactions are used for operational characterization of the kinetic stability of the metal species of interest. These experiments imply that although metals bind rapidly to humic acid, the aqueous-phase metal humate complex formation reaction is still proceeding over a long period of time (up to several years) which promotes formation of more stable complexes and retarded subsequent dissociation. In general, increasing pre-dissociation equilibration time decreases Th-HA complex dissociation rates. Increasing Th/HA ratio increases Th-HA dissociation rates. Overall results indicate that Th-humic acid binding strength increases with increasing temperature. A separate experiment investigates the competition between Th and Am for generation of humate colloid-borne actinides. The Th-Am competition experiment performed at quite low actinide concentrations shows significant effects of Th in reducing Am-HA binding strength. Thus Am(III) is desorbed faster in presence of Th(IV). In contrast, the desorption kinetics of Th(IV) complexed with HA does not change in presence of Am(III). The lability of the Am(III) humate complexes in the presence of Th(IV) is the result of a successful competition of Th with Am for strong binding sites of the humic acid. The ligand exchange reactions are shown to be an efficient method for the specification of labile and inert metal species in aquatic HS samples.

In the third part of the work, we examine the resistance of HAS colloids and colloid-borne actinides relative to changes which are likely to occur in natural open systems, namely dilution, variations in pH, temperature, occurrence of ligands such as EDTA and humic acids, presence of cations such as Na^{+}, Ca^{2+}, and $Al(OH)_x^{3-x}$. The stability of HAS colloids and colloid-borne actinides are monitored by determining the monomeric silica concentration and colloid-borne Am or Th fractions versus time. The colloidal solutions are prepared by titrating an acidic solution, containing varying concentrations of metal ions (Al(III), Eu(III), Am(III), Th(IV)), with a basic solution, containing silicate ions, to a pH~9. The resulting suspensions are aged for different times and then diluted in Milli-Q water in proportion 1:100. A small aliquot of HA stock solution is introduced to the colloidal solution immediately after its dilution to give a final HA concentration varying from 0 to 10 mg/l. The results show that stable HAS colloids might exist in water solutions at the naturally relevant concentration of silicon and aluminium at circum - neutral pH. HA influence silica dissolution rates indirectly, primarily through their complexation with aluminium and other metal ions. The initial rates of dissolution are several times greater than the rates after one or more days depending on the pre-equilibration time before dilution. A similarly rapid time-scale is observed also in the early portions of EDTA-induced dissolution experiments. Increasing the aging time and / or enhancing the sample temperature stabilize HAS colloids and the actinide - colloid binding. The simultaneous presence of HA and HAS is found to enlarge the region of colloids stability.

1 Introduction

The role of colloids in the migration of radionuclides in the geosphere has been emphasized in the performance of the long-term safety assessment of waste repositories. Aquatic colloids are omnipresent in natural waters [3] and composed of inorganic elements with different oxidation states via oxo-bridging [4] or inorganic-organic composites in which ubiquitous humic acid is normally involved [5-7]. Their chemical composition, number density and particle size distribution vary depending on the geochemical conditions of their provenance. Hence, in natural systems the particle size distribution has been generally observed between 1 nm and up to 100 nm, but very often below 50 nm [8]. For this size range, the typical number density has been reported to vary between 10^8 to 10^{14} particles/l water [5, 8]. Regardless of their composition, aquatic colloids have been recognized to play a significant carrier role in the migration of trace contaminants including radionuclides in aquifer systems [8, 9]. Several investigations have demonstrated that low soluble, surface reactive radionuclides could travel much faster than anticipated from traditional solute transport models taking into account the thermodynamic solubilities [10-12]. In all cases the enhanced radionuclide transport has been attributed to the association of contaminants with the mobile colloidal phase. As highly charged cations, actinides manifest strong tendency towards hydrolysis / polynucleation and complexation, and hence, high potential for incorporation into aquatic colloids [8, 13]. Numerous studies have concentrated on the actinide interaction with aquatic colloids [7, 14-17], however the process for formation of aquatic colloid-borne actinides is still not well understood, a key issue being the stability of such colloids [7]. Therefore, the appraisal of colloid-borne actinide generation is necessary for a possible prediction of the colloid-facilitated migration of actinides which is a requirement for the long-term safety analysis of nuclear waste repositories.

Hydroxyaluminosilicate (HAS) colloids are known to be kernels for a variety of aquatic colloids [8, 18-20], as Al and silicic acid are always present in natural water and may undergo co-nucleation via oxo-bridging to form stable water-soluble composites [3]. In the course of HAS-colloid formation, trace elements are easily integrated in the conucleation process and become colloid-borne species. This process has been recently investigated for tri-and tetravalent actinides [1, 2, 21, 22]. The present work is a continuation of this series and pursues aspects regarding the stability of the HAS-colloid-borne actinides. For a better approach to the complex natural conditions, the formation of HAS-colloid-borne actinides

is further analyzed in the presence of humic acid (HA). As humic acid is an ubiquitous component of natural waters and has a strong affinity to complex metal ions of higher charges ($z \geq 3+$) [7, 13, 23], its impact on the formation of HAS colloids and hence of HAS-colloid-borne actinides is expected to be significant.

The selected actinides are Am(III), Th(IV), Np(V) and U(VI). Am, Np and U are the actinides of concern from the radiological point of view, due to their long-lived isotopes and large abundance in the spent fuel to be disposed. Due to its stable oxidation state, Th(IV) is taken as a model element to characterize the behaviour of redox sensitive actinides like Pu, U and Np which may be reduced to the tetravalent state at low redox potential in the near field of a nuclear repository [24].

2 Experimental

Ultra-high purity, double deionized water, provided by a MiliQplus® system (18.2×10^{-6} $\Omega \cdot cm^{-1}$) is used in the experiments. Working solutions are prepared daily by diluting the stock solutions. All experiments are open to the atmosphere.

2.1 Preparation of inactive and radioactive stock solutions

MOPS buffer stock solutions

0.05 M MOPS (3(N-morpholino) propanesulfonic acid) buffer solutions are prepared by dissolving the free acid in deionized water and neutralizing with 1 M NaOH to pH 6.6, 7.2 and 7.8.

EDTA stock solutions

0.1 M EDTA stock solutions of pH 5, 7 and 9 are prepared by dissolving the disodium salt of the ethylenediamine tetraacetic acid (Merck) in 0.1 M NaOH followed by pH adjustment with 0.1 M HCl. The concentration of EDTA stock solutions are checked by spectrophotometric titration with Ca(II) using Eriochrom Black T as a metal – lochromic indicator.

Chelex 100

The functional groups of the resin are iminodiacetic acid (IDA) bound to a polystyrene backbone, and the exchange capacity amounts to 2.1 mequiv/g dry weight. Purification of the chelating resin and conversion into a mixed H^+/Na^+ form are made by first rinsing with 1 mol/l HNO_3, washing with 0.5 mol/l NaCl until the pH of the solution is near-neutral, and finally percolating with Milli-Q water through the chelating resin in order to remove

excess NaCl [25]. This pretreatment is selected to obtain a mixed Na^+ and H^+ resin form. The purified ion exchanger resin is dried at 45 °C.

Al stock solutions

Al stock solutions of: $2x10^{-5}$, $2x10^{-4}$, $4x10^{-3}$ M Al in 0.03 M HCl and of $2x10^{-2}$ M Al in 0.04 M HCl are prepared by appropriate dilution of an Al solution (ICP standard, Aldrich) containing 0.37 M Al in 1.23 M HCl, with HCl 0.1 M and deionized water.

Si stock solutions

Two sets of stock solutions are prepared for the present experiments, following two approaches:

(1) Solutions of $2x10^{-4}$, $2x10^{-3}$, $2x10^{-2}$ M Si in 0.03 M NaOH, and of $2x10^{-1}$ M Si in 0.2 M NaOH. These solutions are prepared starting from an initial Si solution (ICP standard, Aldrich) containing 0.3489 M Si in 0.83 M NaOH, which is diluted and adjusted for pH with HCl or NaOH, to a final pH of approximately 12. The solutions remain under-saturated relative to the solubility concentration of amorphous silica and thus Si is present as monosilicic acid in the stock solution.

(2) Solutions of $4.2x10^{-2}$ M Si in 0.01 M MOPS buffer solution at pH 6.6, 7.2 and 7.8. The solutions are obtained by neutralization in MOPS buffer of a solution containing 7.0 M Si in 4.0 M NaOH (Aldrich). The initial alkaline Si solution, in which monosilicic acid prevails, is diluted directly to the neutral pH range. Thus, the solution becomes oversaturated ($4.2x10^{-2}$ M Si corresponds to 21 times the solubility concentration of amorphous silica) leading to instantaneously polymerization of the monosilicic acid [21].

Eu, ^{232}Th and ^{238}U stock solutions

Several actinide (or lanthanide as analogue) stock solutions are prepared from either europium nitrate, thorium (^{232}Th) nitrate AAS standard solutions (Aldrich Chemical), or uranyl (^{238}U) nitrate salt (p.a. Merck). Suprapure HCl is used for dilutions.

^{241}Am, ^{234}Th, ^{237}Np and ^{233}U stock solutions

Radioactive solutions of ^{241}Am, ^{237}Np, and ^{233}U are provided by the INE Karlsruhe as well as by the Institute of Radiochemistry (RCM) Munich and are used without further purification. Stock solutions of 8.0×10^{-5} M ^{241}Am in 0.1 M HCl, 2.4×10^{-3} M ^{237}Np in 0.1 M HCl and 5.0×10^{-4} M ^{233}U in 0.1 M HCl are prepared by acidic dilutions of the original solutions.

^{234}Th is prepared in the laboratory from natural uranium in two consecutive steps [22]:

(1) 25 g $UO_2(NO_3)_2$*6 H_2O (p.a. Merck) is brought to the chloride form, UO_2Cl_2, by addition of conc. HCl, evaporation to dryness, dissolution in 8 M HCl and applied to a column (4.4 cm diameter, 72 cm length) filled with 750 ml of the anion exchange resin Dowex 1X8 (100-200 mesh). Th(IV), unlike U(VI) and Pa(V), does not form chloro-complexes and is eluted with 8 M HCl. The eluate is evaporated, dissolved in concentrated HNO_3 and H_2O_2 and evaporated three times until all organics are destroyed. The residue is dissolved in 8 M HNO_3 for the second purification step. (2): The hexanitrato complex of Th is sorbed onto a small column filled with 80 µl anion exchange resin Dowex 1X8. The remaining U and Pa impurities are washed out with 8 M HNO_3. Th is eluted with 8 M HCl. The eluate is evaporated several times with concentrated HNO_3 to dryness and re-dissolved in 0.8 M HNO_3 resulting in approximately 1.5×10^4 Bq ^{234}Th. It should be noted that when ^{234}Th is used as a tracer and the radioactive measurements are carried out by LSC, its daughter ^{234m}Pa is also measured as well, as the decay is as follows:

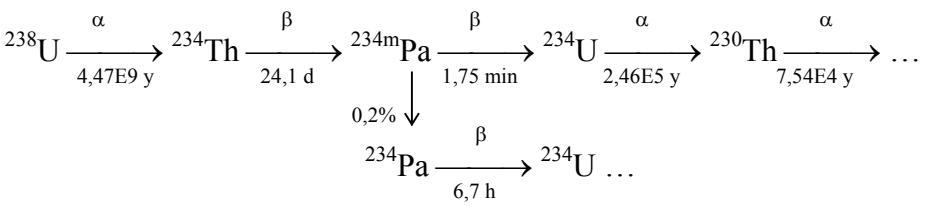

Humic acid stock solution

Natural humic acid, originating from the groundwater of the bore hole Gohy-573 in the Gorleben aquifer (Germany) is used for the experiments. The humic acid was isolated, purified and characterized by Buckau et al. [26], following the procedure by NaF treatment, repeated precipitation with $HClO_4$/dissolution with NaOH and freeze drying. The proton exchange capacity, measured by potentiometric pH titration is of 4.82 ± 0.05 meq/g.

Inactive HA stock solutions are prepared by dissolving the purified Gohy-573 humic acid provided by INE Karlsruhe [26] in 0.1 M NaOH and neutralizing to pH of ~ 7 by addition of 0.1 M HCl. It is found that no buffer is needed and the pH stays within ± 0.1 units for at least two months.

In order to trace the behavior of the humic acid, we use ^{14}C-labelled humic acid. The ^{14}C-labelled humic acid (purified Gohy-573) stock solutions of 4.4 ÷ 4.8 g/l are provided by the Institut für Isotopen Forschung IIF-Leipzig.

The radiolabelling was performed by A. Mansel [27] via diazotization and azo coupling reactions. The aniline ^{14}C-labelled hydrochloride (Amersham) is converted with sodium nitrite to diazonium ion in a hydrochloride solution at 0^oC. The diazonium ions react with the activated aromatic residues of the humic acid at pH ~ 9 and 0 - 5^oC. The resulting product is again purified and characterized by size exclusion chromatography. The specific activity of the ^{14}C-labelled HA (solution of pH 6.5) is in the range of (1.68 ÷ 1.76) x 10^8 Bq/g. The labelling procedure is published elsewhere [27].

2.2 Mother solutions for actinide/colloids interaction

All coprecipitation experiments are carried out at room temperature (21 ± 2 °C) and atmospheric pressure. Calibration of the pH-meter is performed using buffer solution standards and the accuracy of pH measurements is of ± 0.03 pH units. Magnetic stirring is applied during the coprecipitation reaction. All coprecipitated samples are stored in tightly closed polyethylene bottles and conditioned for time period from 1 h to 800 d. The reproducibility of the coprecipitation experiments is found within 10 % (1σ).

HAS colloids

A typical 40 ml coprecipitation sample is prepared by titrating 20 ml Al stock solution containing an aliquot of the acidic stock solution of the radionuclide under investigation and eventually the actinide or lanthanide carrier, with a 20 ml Si solution (stock solutions 1 as described in section 2.1). The actinide participates in the co-nucleation of Al and Si, i.e. the actinide interacts with HAS in 'statu nascendi'. The coprecipitation is carried out to a preset pH with the aid of an automatic titrator (736 GP Titrino, Tinet 2.4 software, Metrohm). By the coprecipitation procedure, different combinations of Al/Si concentration ratios are prepared at the initially preset pH values of 4.0, 5.0, 6.0, 7.0, 8.0, 9.0. The Al concentration is varied between 0, 10^{-5} and 10^{-4} M, that of Si between 0, 10^{-3} and 10^{-2} M. At 10^{-3} M Si, the solution remains under-saturated and monosilicic acid prevails. At 10^{-2} M Si, the initial alkaline solution (containing monosilicic acid) becomes oversaturated by neutralization during the coprecipitation experiment, which leads to the formation of polysilicic acid. HAS mother solutions of 10^{-5} M Al/ 10^{-3} M Si generate the HAS-monosilicic acid colloids, those of 10^{-4} M Al/ 10^{-2} M Si generate the HAS-polysilicic acid colloids.

The Eu, ^{232}Th, and ^{238}U solutions are used with trace amounts of actinides (^{241}Am, ^{234}Th and ^{233}U) in experiments involving higher actinide concentrations. Eu is added for final Am+Eu concentration above $5x10^{-8}$ M; ^{232}Th, for final Th concentration above $2x10^{-12}$ M, and ^{238}U for final concentration of U above $8x10^{-6}$ M. A similar coprecipitation procedure of Si and Al, but without actinide addition, is carried out for the preparation of HAS mother solutions, which are then conditioned for variable time periods.

HA colloids

Samples of 40 ml mother solutions containing adequate amounts of the actinide and Al stock solutions and variable amounts of ^{14}C-labelled HA, are prepared in MOPS buffer at pH 6.6, 7.2, and 7.8. In some experiments the Al solution is replaced by solutions of either: Eu, ^{232}Th, or ^{238}U. For experiments regarding Th, two sets of samples are prepared in each case: either with ^{234}Th (and ^{232}Th) and unlabelled humic acid to monitor Th behaviour, or

^{232}Th and ^{14}C-labelled HA for monitoring the humic acid. A high number of mother solutions for parameter screening experiments are generated from different combinations of several parameters: the final concentration of Al lies between 0 and $1x10^{-5}$ M, the Eu concentration is $1x10^{-5}$ M, Th concentrations varied between $5x10^{-12}$ M and $1x10^{-5}$ M and those of U between $3x10^{-7}$ M and $1x10^{-5}$ M. Humic acid concentration is adjusted between 0 and 10 mg/l. Variable HA / metal ion concentration ratios are generated. This is achieved either by maintaining the metal ion concentration constant and increasing HA concentration, or by decreasing the metal ion concentration while maintaining a constant HA concentration.

HAS + HA colloids

Samples of 40 ml mother solutions are prepared in MOPS buffer by neutralizing the acidic solution containing variable aliquots of the actinide (^{241}Am / ^{234}Th +^{232}Th / ^{233}U stock solution and Al stock solutions, with the Si solution. The Si stock solutions used here (stock solutions 2 described in section 2.1) are especially important for the cases where aluminosilicate colloids are generated from polysilicic acid, in order to overcome the polymerization kinetics the neutralization of alkaline monosilicic acid especially at circum-neutral pH [21]. Thus, the introduction of such a Si solution maintains the polysilicic acid transiently (ca 1 h) to react at once with Al and actinides. After one hour sample conditioning time, an aliquot of the ^{14}C-labelled HA solution is added. As mentioned in the case of humate colloids, for the experiments regarding Th, parallel experiments are carried out. In the present experiment the pH varied from 6.6 to 7.8, Al concentrations were between 0 and $1x10^{-3}$ M and Si concentrations ranged from 0 to $1x10^{-2}$ M. The HA concentration is kept constant at 6.5 mg/l.

2.3 Activity partition between solution, colloids and precipitate

Consecutive filtration and ultra-filtration are performed on the coprecipitated sample for a sequential separation of the precipitate and colloids. The first filtration is made by a membrane filter of nominal pore size of 450 nm (Sartorius) to separate the precipitate fraction. The second filtration is carried out on this filtrate to separate the colloids at a pore size of 10 kDa (approximately 1.5 nm nominal pore size) (Centricon YM-10, Milipore) by

centrifugation in the Biofuge primo Heradeus-Kendro for 1 h at 5000 x g. The activity of the radionuclides ^{241}Am, ^{234}Th, ^{237}Np, ^{233}U, ^{32}Si, and ^{14}C is determined in the filtrates by liquid scintillation counting (LSC) as will be described below. The first filtrate at 450 nm contains both the colloidal and ionic species of the element under investigation. Thus, the difference in the activity of the initial solution and the first filtrate represents the activity of the precipitate. The activity difference between the first and the second filtrate is then ascribed to the colloid-borne species, since the second filtrate from the 10 kDa pore size contains only the ionic species. Because the ultrafiltration methodology is operationally defined, it is imperative that any uncertainties due to experimental artefacts are, as far as possible, identified to permit the accurate interpretation of the data. Obviously, the quantity of colloids deduced from the difference of concentrations found in both filtrates does not represent a conservative estimate for colloid formation but this quantity, however, can be used in relative terms as a measure to compare the colloid concentration in different samples and especially to observe the time dependent changes. In addition to sorption to the walls of the ultrafiltration assembly and membrane, the separation process in ultrafiltration is dependent both on pressure and concentration gradient. As can be appreciated from Figure 1, as the volume of solvent in the cell decreases the concentration of HA in the molecular fraction increases as a result of a breakthrough of larger-molecular-size solutes. Therefore, for comparative measurements, it is important to use the same volume and centrifugation force.

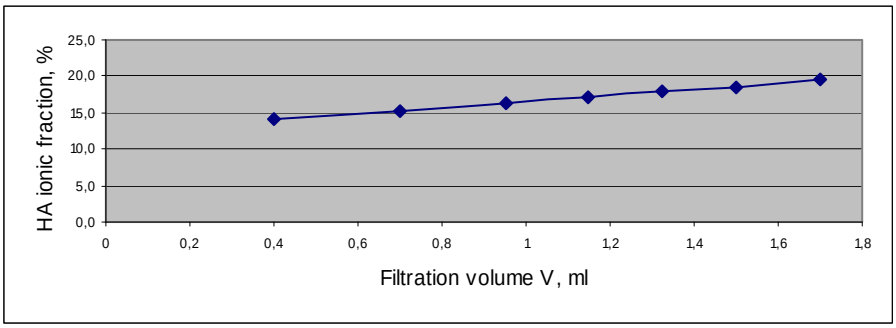

Figure 1 The influence of the filtration volume of continuous ultrafiltration using a Centricon YM-10 ultrafiltration unit on the permeate concentration of HA; 2 ppm HA in 0.1 M NaOH solution.

Determination of the activity of ^{241}Am, ^{234}Th, ^{237}Np, ^{233}U, ^{32}Si, ^{45}Ca and ^{14}C by LSC

The activity in the samples is measured using a Tri-Carb 29000 CA (Canberra Packard) Scintillator Analyzer. The measurements are performed in antistatic – polyethylene vials of 18 ml volume. 1 ml filtrate samples are mixed with 10 ml Hionic Fluor (Perkin Elmer) cocktail and measured to a preset statistic precision (2σ) of 0.5 %. In the case of ^{241}Am the alpha counting window is 150 – 400 keV. A fraction of about 99 % of the ^{241}Am total counting rate (in the 0 – 2000 keV) is found in the above mentioned alpha counting window. ^{234}Th is measured together with its daughter, ^{234m}Pa, whose short half-life allows the secular radioactive equilibrium to be reached in about 5 minutes. An energy window of 0 – 1000 keV is used for counting. The ^{234}Th counting rate is always corrected for decay relative to the beginning of the experiment. In the case of ^{237}Np, the contribution of the beta tailing activity of the daughter ^{233}Pa into the alpha-energy region of ^{237}Np is separated using the pulse decay analysis option of the scintillator analyzer according to the procedure described by the Packard manufacturer. The discriminator setting is established using ^{241}Am and ^{45}Ca standard solutions with composition and geometry similar to that of the samples. A Pulse Decay Discriminator (PDD) of 120 is chosen as discriminator setting in order to minimize the spillover of beta events into the alpha counting window. The beta counting window is set as 0 – 2000 keV and the alpha window as 140 – 350 keV. For these counting windows and the chosen PDD the beta spillover into the alpha window is below 0.1 %. ^{233}U is measured in the 120 – 400 keV energy window, where approximately 98 % of the ^{233}U total counting rate is recorded. For the dual-labelled samples (i.e. actinide - ^{14}C-labelled HA samples), the degree of overlap between the ^{14}C low maximum energy (156 keV) and the alpha energy region of ^{241}Am or ^{233}U can be resolved manually, by choosing appropriate energy windows. Selection of the windows is achieved by measuring reference solutions containing only the radionuclide of interest, i.e. either ^{241}Am, ^{233}U or ^{14}C and calculating the degree of spectral interference in the counting windows. The ^{14}C counting window is set as 0-120 keV. The alpha counting windows are 150 – 400 keV for ^{241}Am and 120 – 400 keV for ^{233}U. In the beta counting window (0 – 120 keV), ^{241}Am is found to contribute with about 0.5 % of its counting rate in the alpha window, whereas the ^{233}U contribution is found to be of approximately 1%. In all cases the counting rate in the beta window is corrected. Due to the interference of the low energetic beta emitters ^{234}Th and ^{14}C the simultaneous measurement of the two radionuclides is not possible by LSC. Therefore, parallel samples are prepared labelled either with ^{234}Th or ^{14}C. Aliquots of the radioactive solution used for spiking are measured along with each set of samples and are considered as reference input activity. Blanks consisting of 1 ml 0.1 M HCl and 10 ml

scintillation cocktail are also measured and the sample counting rate is corrected accordingly.

2.4 Colorimetric quantification of Si and Al

Monomeric silicic acid

Monomeric silicic acid is quantified by the molybdenum test (Spectroquant® 1.14794 Silicon, Merck). The colorimetric method is based on the selective detection of monomeric /dimeric silicic acid species, the so-called soluble silica, reacting fast with the molybdic acid as compared to the oligomeric (colloidal) species. The method uses the reaction between silicate ions and ammonium molybdate forming a silicomolybdic complex which is further partially reduced to the silico-molybdenum blue form. The latter complex shows maximum absorbance at 820 nm. Measurements are performed in 10 mm plastic cuvettes using a Cary 5000 spectrophotometer assisted by the Cary WinUV 3.0 Software. An optimum in precision of the method within 1% (1σ) is obtained between E (extinction) = 0.07 to 3.5, corresponding to the concentration range of 0.1 to 5 mg/l Si. A good linearity is obtained in the region 0.005 – 5.0 mg/l of the silicon concentration.

Soluble Al

In the present work the soluble Al is defined as the Al in a solution passing a 10 kDa pore size filter (after removal of precipitate and colloids) and that can be measured by colorimetry using Chromazurol S as complexation agent (Merck Standard Procedure, Spectroquant 1.14825-Al). The Al-Chromazurol complex has a maximum absorbance at 548 nm. In case that Al is present in solution complexed with EDTA, an additional preparation step is required in order to destroy the Al-EDTA complex (see appendix). Thus, prior the Chromazurol addition the samples are mixed with an acidic solution of 1.5 M $Pb(NO_3)_2$ in 0.1 M HCl for a final Pb concentration in the sample ten fold in excess relative to EDTA and hundred fold in excess relative to the aluminium concentration. The exchange reaction between the EDTA complexed-Al and Pb^{2+} ion is found to be complete within 1 h at pH 1 and ambient temperature. Measurements are carried out in 10 mm quartz cuvettes using a Cary 5000 spectrophotometer assisted by the Cary WinUV 3.0 Software. Al determination is possible in the linear range of $7x10^{-6}$ M up to $1x10^{-4}$ M. The precision of the method is approximately 2 % (1σ). More details are given in the appendix.

3 Results and discussion

3.1 Humic acid (HA) as colloids: influencing parameters

Effects of pH, temperature and HA concentration

Humic acids are operationally defined from the extraction procedure of humic substances (HS) as the insoluble fraction at acidic pH (pH < 2) [26]. They are composed of heterogeneous components with a wide range of molecular weights, size and different chemical moieties and it is also known that the chemical environment influences the aggregation of humic macromolecules [23, 28]. Therefore, the influence of the pH, temperature and of the concentration of humic acid itself on its partition between the precipitate, colloids and solution is investigated.

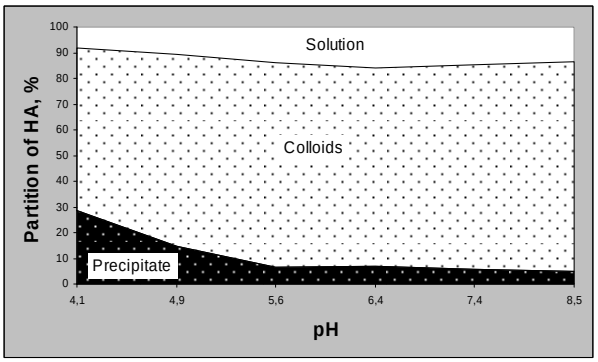

Figure 2 [^{14}C]-humic acid activity fraction (%) normalized to the initial activity in the precipitate, colloids and solution, as a function of pH at contact concentration of 6.5 mg·l^{-1} HA. Results represent values obtained after 35 d sample conditioning time without addition of MOPS buffer solution.

For this purpose, two series of purified ^{14}C-radiolabelled humic acid (Gohy -573) are subject to sequential filtrations, followed by determination of the ^{14}C-activity partition between the solution, colloids and precipitate phase (see section 2.3). The concentration range corresponds to the HA level generally encountered in natural waters, however, one should mention that the maximum concentration used is limited by the strong quenching caused by HA in LSC. In one sample series the HA concentration is kept constant at 6.5 mg/l and the pH is varied from 4 to 9. The results of the pH dependency are shown in Figure 2. A slightly elevated precipitate fraction is observed at pH < 5.5 due to the beginning of the protonation of the HA functional groups leading to aggregation. In the neutral pH region, the fraction regarded as humic colloids after sample conditioning time of 35 days is found to reach approximately 65 – 70 %. At longer conditioning time, however, slightly elevated precipitate and ionic fractions are observed as can be appreciated from Figure 3.

In another sample series the pH is kept constant at 6.6 or 7.8 in 0.01 mol·l^{-1} MOPS buffer solution and the HA concentration is increased from 0.6 to 10 mg/l. A variation of the HA concentration was found to have only negligible effect on the partition of HA. The result

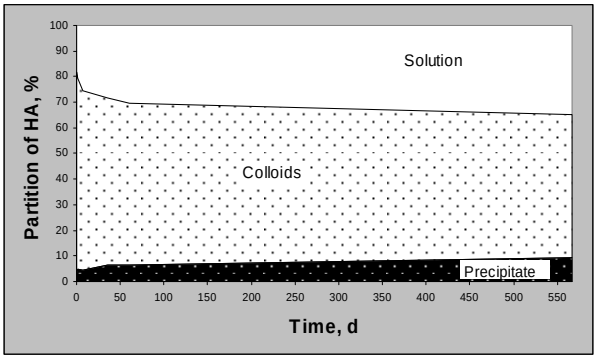

Figure 3 Partition of HA after dilution of 4400 ppm stock solution to 6 ppm in 0.01 M MOPS buffer solution at pH 7.8. Results represent values obtained immediately after dilution and 1, 3, 7, 35, 60 and 570 days thereafter.

suggests that the operating conditions are adequate to exclude excessive coating or clogging of the membrane and allow unrestricted passage of ions and ligands through the ultrafilter. However, at the higher HA concentration, namely 300 mg/l, only 4% of humic acids pass through a 10 kDa membrane probably due to a thicker foiling layer formation and pore blocking.

The time evolution of a colloidal suspension is examined by performing the experiment using a mixture of the inactive humic acid solution with pre-filtered ^{14}C-radiolabelled active humic acid solution. Two different solutions are prepared: 1. The ^{14}C-radiolabelled humic acid solution that has been first pre-filtered through a 10 kDa molecular weight cut-off ultrafiltration membrane (Centricon YM-10, Millipore) is diluted with MiliQ-water to a concentration of 7 mg/l; and 2. The ^{14}C-radiolabelled humic acid solution that has been first pre-filtered through a 10 kDa molecular weight cut-off ultrafiltration membrane is diluted with MiliQ-water and mixed with the inactive HA solution to give a final concentration of 7 mg/l. The solutions should contain a different amount of the smaller molecular weight HA species. After the conditioning time varied from 1 h to 90 days, the filtration process is performed on the samples to separate the large humic acid aggregates and ^{14}C-activity partition between the solution, colloids and precipitate phase is determined. The ^{14}C-activity fraction for both samples that passed through a 10 kDa membrane is shown in Figure 4.

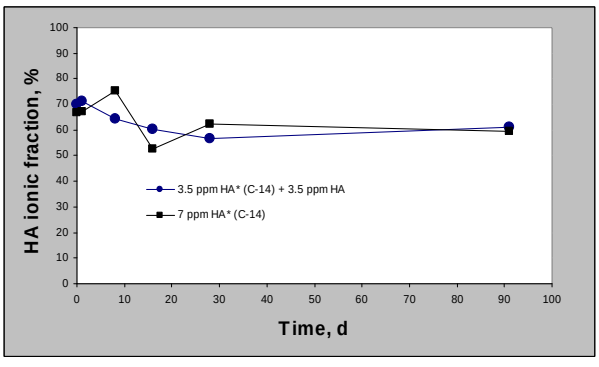

Figure 4 Soluble ^{14}C activity fractions (%) of the pre-filtered active HA solution normalized to the input activity as a function of conditioning time.

The result is that only ≈ 60 – 70 % of the pre-filtered humic acids pass through the filtering membrane again. The soluble ^{14}C-activity fraction is slightly fluctuating from the mean value and shows no clear trends. Hence, it appears that the ultrafiltration technique applied here can not be used to separate the so-called "dissolved" compounds from the "particulate" material without causing aggregation of the

particles in the ionic fraction. The cascade ultrafiltration improves the separation but not completely. It is obvious that filtration should not be regarded as a sieving process except when very large pore filters are used. The self-coagulation of the humic macromolecules may occur at the membrane surface. Moreover, the humic acids are not spherical, uncharged solute molecules and macromolecules that passed through a membrane for the first time might be retained later on. Also, the association of the humic macromolecules that passed through a 10 kDa membrane may occur already in the course of centrifugation at 5000g.

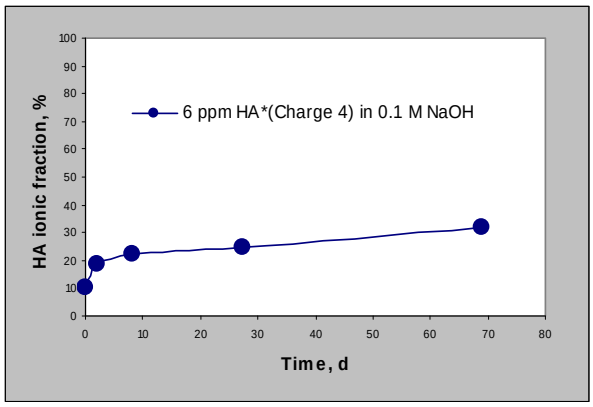

Figure 5 Degradation the HA colloids in 0.1 M NaOH. Soluble ^{14}C activity fraction (%) normalized to the input activity as a function of storage time.

In the additional experiment, the colloidal HA fraction is separated from the large and small molecular weight HA species and then NaOH is added to get a final HA concentration of 6 mg/l. The dissolution of HA is monitored in 0.1 M NaOH as a function of time. The data are depicted in Figure 5. It would appear that a mild alkaline hydrolysis takes place, and that low molecular weight HA species could be liberated by breaking hydrogen bonds. In addition the electrostatic repulsion between the membrane surface and HA and between HA in solution and deposited HA is enhanced in alkaline medium. These phenomena induce a reduction in adsorption of the humic acid on the membrane surface as the pH increases. Nevertheless, one should mention that 65 – 70 % of HA is not able to pass through a 10 kDa membrane even after 70 days conditioning time with 0.1 M NaOH at 4ºC.

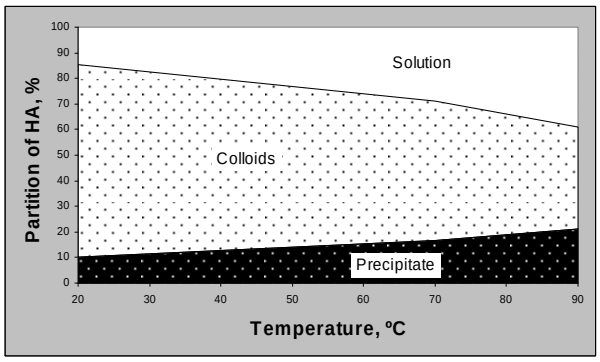

Figure 6 Partition of HA in 0.01 M MOPS buffer solution at pH 7.8 as a function of temperature. Solutions are kept in water bath for 4 days storage at 23ºC, 50 ºC, 70 ºC and 90ºC and then cooled down at room temperature again for 4 days.

The impact of temperature on the stability of the HA is studied with solutions of 6 ppm HA at pH 7.8 (10^{-2} mol·l^{-1} MOPS buffer). Solutions are kept in water bath for 4 days storage at different temperatures up to 90ºC. The difference between UV/Vis absorption of HA solution stored at room temperature and the absorption of the HA solution stored at 90ºC is small (ca. 3.6 % at 254 nm) but

well reproducible. At 90ºC, the spectrum shows a slight change with increase towards shorter wavelengths. This indicates that the aggregation of HA occurs that induces the increase in the UV absorbing properties of HA. The fractionation tests demonstrate that HA colloids dissolve and precipitate at the same time as in the case of long pre-equilibration time (cf. Figure 6 and Figure 3). The result shows that rearrangement of HA takes place already at 40ºC. With increasing temperature the expected increase in conversion velocity is found.

Effect of metal ions

It has been known since the earliest studies that humic substances form insoluble salts with a wide range of metal ions. Many di-, tri-, or tetravalent ions will bring about the precipitation of a greater or lesser amount of humic acid from solution. Therefore, the effect of Ca, Al, Eu and Th at 10^{-5} mol·l^{-1} concentration on the destabilization of humic colloids is examined by adding metal chloride solution to gradually increasing amounts of HA at pH 6.6 and 7.8. The samples are left then to stand undisturbed at room temperature in tightly closed PE-bottles over a period of one week. The selected results for pH 6.6 are

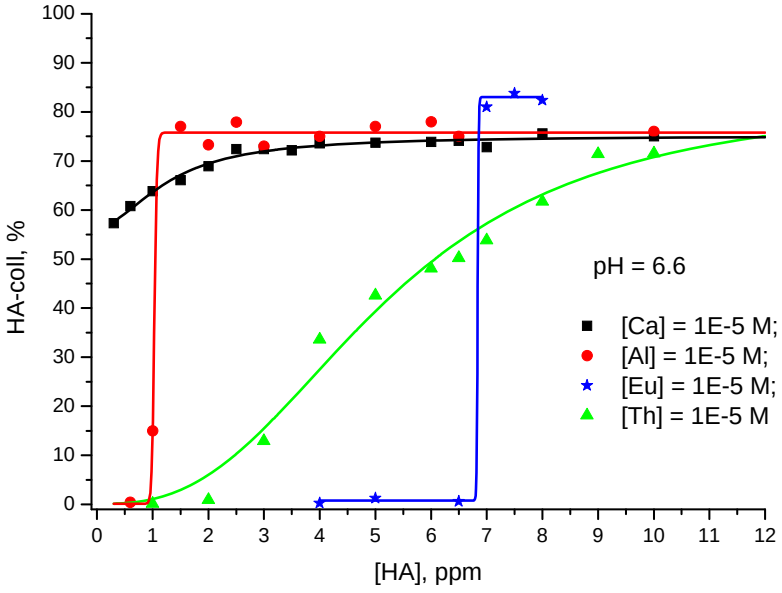

Figure 7 Effects of di-, tri- and tetravalent cations on the [^{14}C] – humic acid activity fraction in colloids as a function of humic acid concentration in a solution of pH 6.6. Results represent values obtained after 7 days sample conditioning time.

illustrated in Figure 7. Addition of di, tri- and tetravalent ions leads to complete or partialdestabilization and precipitation of the HA colloids at low HA concentration . The point of HA precipitation informs us about the amount of HA that can possibly complex

with the introduced amount of metal species. If we compare first the trivalent metal ions we shall see that the threshold concentrations for aggregation of HA are different: here, aggregation starts only at 6.5 mg/l HA for Eu, compared roughly to 1 mg/l HA for Al. The difference can be explained by a competition reaction with hydroxyl ions that is significant

in the case of aluminium. By further increasing the HA concentration, the precipitate is promptly transferred to the colloidal phase. The Th system shows two distinct differences from the Eu and Al systems. Firstly, one needs higher HA concentration (i.e. about 10-12 mg/l HA) in order to reach a fraction of about 70 % C-14 activity in the colloidal phase

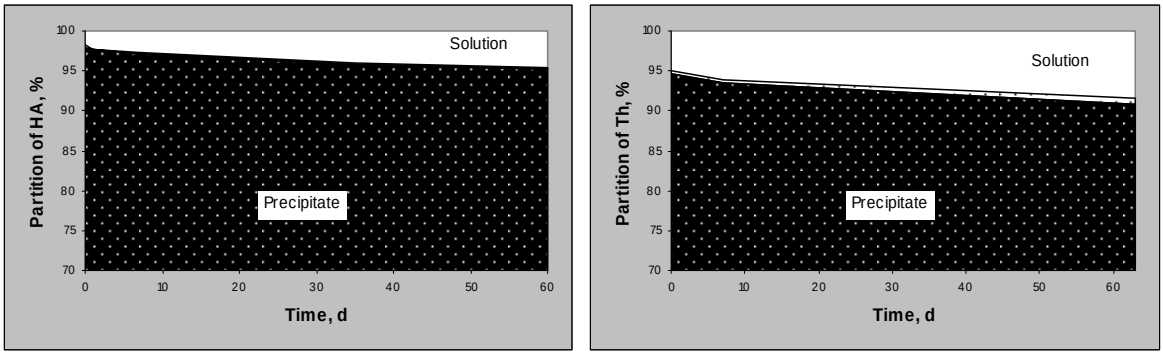

Figure 8 [^{14}C] – HA and ^{234}Th activity fractions in the precipitate, colloids and solution, as a function of the sample conditioning time in a solution of pH 6.6 containing 1 mg·l^{-1} HA and 1x10^{-5} mol·l^{-1} Th.

comparable to the colloidal fraction of pure HA shown in Figure 7. However, the most noticeable difference is that Th appears to have the higher range of concentration from the onset of aggregation to the point where aggregation is complete. Agglomeration of HA occurs relatively slowly and precipitation of HA is not complete even after 2 months reaction time. On the contrary, the percentage of Th in the colloidal phase varies only slightly already after 1 day reaction time. The formation of colloids, with molecular size between 2 nm and 0.45 μm, accounts for a thorium concentration approximately three orders of magnitude higher than the solubility of the amorphous thorium hydroxide at pH 7.8. Hence in natural system, Th will be associated with particulate or colloidal HA present in ground water and its chemistry will be not controlled anymore by the precipitation of a single mineral phase. Furthermore, Th and Am seem to favour complexation with the high molecular weight HA species over smaller humic acid molecules since the actinide fraction in colloids surpass the ^{14}C activity in the colloidal phase. However, all experiments show that even at higher metal concentrations, provided that there is some humic material remaining in solution, there is always some low weight material present. One example of the formation of Th-humate complexes is illustrated in Figure 8. ^{234}Th and ^{14}C activities are found only in the precipitate and solution. The colloidal fraction has almost vanished.

Divalent Ca ions show less influence on the HA colloid stability and the aggregation process occurs relatively slowly: within one or two months. Moreover, even 0.08 mg/l HA colloids are not precipitated completely in presence of 10^{-5} mol·l^{-1} Ca and only a maximum of 30 % Ca is found to be associated with the HA colloids at whatever concentration ratio

of HA to Ca. The obtained results indicate that for any given pH, HA possesses the ability to hold tri-, tetra and hexavalent cations in higher amounts than weakly coordinated divalent calcium ions if the metal concentration does not exceed the proton exchange capacity of HA.

When increasing pH to 7.8, we observe that the conversion of the precipitate to the colloidal phase starts at lower HA concentration, as compared to pH 6.6. It seems that increasing pH increases the quantity of metal ions bound by HA since with increasing pH deprotonation of humic acid functional groups takes place and more sites become available for complexation. Also, the metal hydrolysis advances with increasing pH. For this reason, the observed shift to lower HA concentration with increasing pH might be correlated to a lower positive charge carried by the ionic species at this pH as for pH 6.6 According to the metal ion charge neutralization model, describing the metal ion-humate complexation, a lower positive charge requires less amount of HA for complexation, or in other words, there is less positive charge available for neutralization and precipitation of humic acid.

The higher valence cations form bridges between anionic groups of different humic macromolecules and thereby enhance their associations. This allows the macromolecules to approach one another more closely, so that intermolecular attractive forces predominate and coagulation or precipitation can occur more effectively.

3.2 Stability of humic colloid-borne actinides

The stability of actinide binding to colloids is one of the relevance criteria for their colloidal facilitated migration. Stable incorporation of actinides into stable aquatic colloids promotes the colloids as carrier for actinide migration with the water flow without substantial geochemical hindrance. Stability of actinide-colloids binding refers to the actinide ability to remain as colloid-borne species upon changes in the environmental conditions. Therefore, the binding stability is operationally defined by the selected conditions like variations

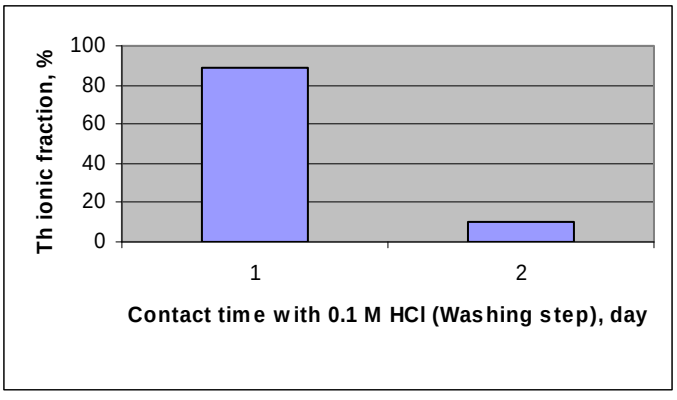

Figure 9 Desorption of 5.5×10^{-6} mol·l^{-1} Th from 6.5 mg·l^{-1} HA colloids with aid of 0.1 M HCl.

in pH, temperature, ionic strength, the presence of anionic ligands, as potential changes that may occur in the natural environment. The present work considers the stability of the colloid-borne actinides relative to the pH decrease and EDTA as competitive ligand.

pH reversibility

The pH reversibility is tested for actinides bound to HA colloids and aged for 60 days at pH 6.6 and 7.8. After a conditioning time of 60 days, the colloids are separated by ultrafiltration at 10 kDa pore size and washed several times with 0.1 M hydrochloric acid. The contact time with the wash HCl is one day for each desorption step. After each desorption step, the dissolved actinide fraction is separated again by ultrafiltration. The result shows that colloid-borne Th is more stable than colloid-borne Am but even the former one is completely desorbed from HA colloids at pH 1 within 1 – 2 days, suggesting that the colloid-borne actinide species appear to be chemically unstable in the acidic medium. In relation to the initial colloid-borne Th at pH 7.8, the dissolved fraction is given in Figure 9.

EDTA resistance

In order to get a relative assessment of the actinide-colloid binding strength under the condition of maximum formation of colloid-borne actinides, a ligand competition experiment is further carried out, with the aid of EDTA as competitor for the HA since EDTA is a well known chelating agent which forms in solution very stable complexes with most metal ions, including actinides, as becomes obvious from the complexation constants at 20ºC and an ionic strength of 0.1, lg K is $7.4x10^{-17}$ for Al^{3+}, $6.9x10^{-19}$ for Am^{3+}, $3.5x10^{-19}$ for Cm^{3+}, $5.0x10^{-26}$ for Th^{4+}, $1x10^{-13}$ for UO_2^{2+}, and $4.1x10^{-17}$ for PuO_2^{2+}[36].
In the first series of samples, the HA/Th concentration ratio is varied by keeping the concentration of HA constant at 6 ppm and increasing the concentration of Th from $5x10^{-11}$ to $5x10^{-5}$ mol·l^{-1}. After an aging time of 10 days, $5x10^{-4}$ mol·l^{-1} EDTA is added and the distribution of Th in solution, colloids and precipitate is measured as a function of contact time with EDTA. The dissociation kinetic and the apparent equilibrium constants of the exchange reaction are presented in Table 1. The nature of the experiment observing Th-HA complex dissociation allows three operational fractions, based on kinetic behavior, to be defined. The first, rapidly dissociating Th (fraction F1), is that proportion of Th-HA complexes dissociating within 8 hours. The second, slowly dissociating Th (fraction F2), is the proportion of Th-HA complexes whose dissociation reaction occurs during two weeks.

The third, nondissociating Th ([Th-HA]eq), is comprised both of Th in Th-HA complexes which are more thermodynamically stable than the Th-EDTA complex and the Th-HA complexes with very small dissociation rate constants.

Table 1 Kinetic parameters for desorption of Th from 6 ppm HA colloids with aid of $5x10^{-4}$ mol·l^{-1} EDTA at pH=7.8 in 10^{-2} mol·l^{-1} MOPS buffer solution

[Th], mol/l	*Age = 10d*					*Age = 33d*				
	F1, %	*τ1, d*	*F2, %*	*τ2, d*	*[Th-HA]eq, %*	*F1, %*	*τ1, d*	*F2, %*	*τ2, d*	*[Th-HA]eq, %*
$5x10^{-11}$	46	0.1	0	-	54	28	0.107	8.5	3.3	64
$5x10^{-10}$	41	0.08	5	4	54	33	0.13	7.6	5	59
$5x10^{-9}$	42	0.08	12	3.8	46	29	0.090	14	2.2	57
$5x10^{-8}$	37	0.03	26	3.3	37	38	0.13	20	5.0	42
$5x10^{-7}$	57	0.1	21	3.8	22	37	0.05	35	2.9	28
$1x10^{-6}$	59	0.1	22	4.1	19	47	0.095	28	3.7	25
$5x10^{-6}$	63	0.15	23	3.2	14	46	0.17	41	3.5	13
$1x10^{-5}$	74	0.18	20	2.9	6	52	0.24	39	2.6	9
$5x10^{-5}$	73	0.14	25	0.8	2	40	0.27	54	1.1	6

where F1 – fraction of the colloidal Th dissociating with the time constant $\tau 1$, %; F2 – fraction of the colloidal Th dissociating with the time constant $\tau 2$, %; $[Th\text{-}HA]_{eq}$ – final actinide concentration in the colloidal fraction after equilibration time of 100 days. $[Th\text{-}HA] = [Th\text{-}HA]_{eq} + F1 \cdot \exp(-\tau/\tau 1) + F2 \cdot \exp(-\tau/\tau 2)$.

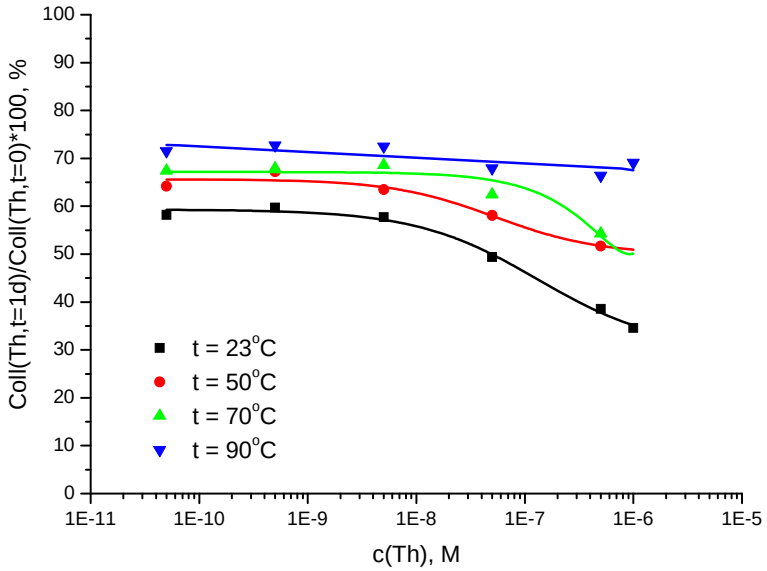

Figure 10 Percentage of Th in colloidal fraction on the next day contact time with $5x10^{-4}$ mol·l^{-1} EDTA normalized to the colloidal fraction on the beginning of the desorption experiment. Pre-dissociation equilibration time for the Th-HA complex = 4 days at 23ºC, 50ºC, 70ºC, and 90ºC

The result for the samples of interest containing colloid-borne Th and subjected to EDTA desorption shows that, as the concentration of Th decreases, the solubilisation of colloid-borne Th by EDTA is hindered through its complexation with HA. The result is supporting the hypothesis about the existence of a minor quantity of strong binding sites and a major quantity of weak binding

sites in the HA. The above metal first occupies strong binding sites and after all the strong binding sites are occupied, the remaining metal is bound to the weak binding sites of the humic acid.

The next experiment intends to study the role of kinetics in the complexation of Th with humic colloids. Therefore, we prepare samples with colloid-borne Th just like before but vary the sample aging time as well as temperature. Table 1 and Figure 10 illustrate the results as follow: increasing the aging time from 10 to 33 days, leads to less solubilised Th, that means to more EDTA-resistant colloid borne Th; enhancing the sample temperature from 23ºC to 50ºC and to 90ºC further stabilizes the Th-HA binding. The result implies that although metals bind rapidly to humic acid, the aqueous-phase metal humate complex formation reaction is still proceeding over a long period of time (up to several years and more). The evidence presented here for a very slow component in aqueous-phase Th-HA complex formation reaction has serious implications for experiments designed to observe metal-humic substance complex equilibrium.

Table 2 Percentage of Am in colloid, ionic fraction, and precipitate as a function of the contact time with Chelex resin. The samples are contained 6 ppm HA, $5x10^{-8}$ mol·l^{-1} Am and/or without $5x10^{-8}$ mol·l^{-1}Th in 0.01 mol·l^{-1} MOPS buffer solution at pH 7.8

Am-241	*Sample contains only Am*			*Sample contains both Am and Th*		
time, d	ppt, %	coll, %	ion, %	ppt, %	coll, %	ion, %
0	1.8	84.4	13.8	1.8	86.2	12.0
0.15	2.8	85.6	11.7	2.6	85.3	12.1
1	4.2	84.4	11.4	5.0	82.8	12.2
6.9	18.6	70.7	10.7	26.5	62.5	11.1
31	56.5	37.2	6.2	77.3	20.5	2.2
60	73.5	22.5	4.0	90.3	8.7	1.0

Table 3 Percentage of Th in colloid, ionic fraction, and precipitate as a function of the contact time with Chelex resin. The samples are contained 6 ppm HA, $5x10^{-8}$ mol·l^{-1} Th and/or without $5x10^{-8}$ mol·l^{-1} Am in 0.01 mol·l^{-1} MOPS buffer solution at pH 7.8

Th-234	*Sample contains only Th*			*Sample contains both Am and Th*		
Time, d	ppt, %	coll, %	ion, %	ppt, %	coll, %	ion, %
0	2.2	85.9	12.0	1.8	89.0	9.2
0.15	1.7	89.6	8.7	1.6	89.5	8.9
1	1.6	89.0	9.4	1.6	89.6	8.8
6.9	1.7	88.1	10.2	0.9	89.3	9.8
31	9.2	80.7	10.1	7.6	85.8	6.6
60	21.8	71.3	6.9	21.4	71.0	7.6

A separate experiment investigates the competition between Th and Am for generation of humate colloid-borne actinides. 0.01 M MOPS buffer solutions with 6 ppm HA and $5x10^{-8}$ M Am or/and Th are prepared under aerobic conditions at pH 7.8. The purified chelating cation exchanger (Chelex 100) is added after 6 days equilibration time. pH is adjusted to 7.8 and monitored throughout the experiment. All samples are kept in tightly closed polyethylene bottles at room temperature and under continuous stirring of the suspension. After different time periods, two filtration processes are performed on the coprecipitation samples for a sequential separation of precipitate and colloids. The results are presented in Table 2 and Table 3.

The Th-Am competition experiment performed at quite low actinide concentrations shows significant effects of Th in reducing Am-HA binding strength. Thus Am(III) is desorbed faster in presence of Th(IV). In contrast, desorption kinetics of $5x10^{-8}$ mol·l^{-1} Th(IV) complexed with 6 ppm HA does not change in presence of $5x10^{-8}$ mol·l^{-1} Am(III). The lability of the Am(III) humate complexes in the presence of Th(IV) is the result of successful competition of Th with Am for strong binding sites of the humic acid.

Table 4 Partition of ^{241}Am and ^{14}C – HA activity in colloid, ionic fraction, and precipitate as a function of the contact time with $1x10^{-3}$ mol·l^{-1} EDTA in a solution of pH 7.8 containing 6 mg·l^{-1} HA, $1x10^{-4}$ mol·l^{-1} Al and $5x10^{-8}$ mol·l^{-1} Am in 10^{-2} mol·l^{-1} MOPS buffer

Time, d	*Am-241 partition*			*C-14 partition*		
	ppt, %	coll, %	ion, %	ppt, %	coll, %	ion, %
0	52	48	0	59	38	3
0.11	2	6	92	8	78	14
0.91	2	2	96	10	74	16
1.9	2	5	93	9.8	74	17

The EDTA resistance of colloid-borne Am and Al is also measured as a function of time. 6 ppm HA is mixed with trace amounts of Am ($5x10^{-8}$ mol·l^{-1}) and $1x10^{-4}$ mol·l^{-1} Al at pH 7.8 and after 1 day conditioning time, EDTA is added at a final concentration of $1x10^{-3}$ mol·l^{-1} (one order of magnitude higher than that of Al, which is in larg excess to the actinide ensuring its complete complexation). The partition of the actinide activity fraction in the three phases is monitored before EDTA addition and at different intervals thereafter. In addition to actinide activity measurements, ^{14}C - labelled humic acid is used in order to facilitate the tracing of humic colloids behaviour. Table 4 gives the results on the actinide and C-14 partition between the three phases as a function of EDTA contact time. As can be seen, the Am activity fraction in the colloidal phase decreases rapidly upon contact with

EDTA. About 90 % of the initially colloid-borne Am is desorbed from the colloids within 2 hours contact time with EDTA. Al is also rapidly desorbed from humic acid, since aluminium ions are responsible for the aggregation of HA colloids observed in the solution phase (see zero time in Table 4) and the addition of the metal chelating ligand EDTA appears to inhibit the aggregation of HA colloids. The experiments show that EDTA successfully competes with HA for binding the trivalent metal ions promoting their fast desorption from humic acid by formation of complexes in solution.

3.3 Hydroxyaluminosilicate (HAS) as colloids

Aqueous hydroxyaluminosilicate colloids may be formed under natural conditions either by condensation reactions or by dispersion from minerals. The most common condensation process occurring in the hydrosphere is the hydrolysis of polyvalent cations (e.g. Si^{4+} and Al^{3+}), the formation of sparingly soluble hydroxides and hydrous oxides and the neoformation of clay minerals at coprecipitation. Colloid formation and stabilization is a very complex process depending on energy barriers and therefore not only thermodynamics but also kinetic factors are involved. The mechanism of HAS formation depends on the concentration of Si and Al, and pH. The process of coprecipitation affected the chemical state of aluminium in amorphous aluminosilicates. For example, the nature of the precipitate can vary widely, even with the same starting solutions, depending on the intensity of agitation at the point of mixing and whether one solution is present locally in excess of the other one [18].

Effect of pH, Si and Al concentrations

We have synthesized HAS colloids in the laboratory at normal temperature and pressure by neutralizing an acidic Al-solution with alkaline Si-solution to a preset pH either in a titration procedure or by mixing with a buffer. In a previous screening experiment [1], several initial concentrations of Si, varying from 10^{-4} to 0.1 M, below and above the Si saturation concentration (ca. $2x10^{-3}$ M), had been combined with varying Al concentrations from 10^{-8} to 10^{-2} M, in the pH range 4 – 9. In an elaborated parameter screening experiment, optimum conditions for HAS-colloid formation had been recognized from their capability to incorporate americium, which had been added in a tracer concentration

as contestant in the condensation process of Si and Al. The optima correspond to mother solutions made at pH 5 – 6 and pH 8 – 9, with a Si/Al concentration ratio Si/Al of 100, but at two different Si concentration levels, namely in a slightly undersaturated and in a 6.5 times oversaturated solutions. The conditions for the formation of monosilicic and polysilicic acid are especially important since polysilicic acid has been shown to have a 10^6 times higher affinity for Al as compared with monosilicic acid [29]. This can be explained as follows: the monomer, $Si(OH)_4$, has a pK_a of about 9.9, but higher, polymerized species have a much lower pK_a approaching 6.7 and hence are more highly ionized than dimeric or monomeric species [18].

The synthetic hydroxyaluminosilicate colloids, generated by coprecipitation in the neutral pH range as described above, had been characterized for particle number density and morphology by several techniques: LIBD (Laser induced break-down detection), AFM (Atomic force microscopy) and SEM-EDX (Scanning electron microscopy coupled with X-ray energy dispersive spectrometry). The HAS colloids prepared out of mother solutions with Si/Al atomic ratios of about 100 appear to be similar to the natural aquatic colloids of protoimogolite / allophane type (precursors of imogolite) in respect with the particle size, shape and Si/Al atomic ratio. They are small colloids (10 – 50 nm) with a low number density (10^{11} – 10^{14} particles/l). The surface characterization of the HAS colloids had been performed by determining of the zero point of charge (pH_{pzc}). The colloids prepared from a mixture of 10^{-3} M Si and 10^{-4} M Al show a pH_{pzc} of 3.53 ± 0.5 [30], which means that the HAS colloids have a negatively charged surface in the pH range of interest (4 – 9) and therefore high potential to migrate with the water flow with little interaction with the geomatrix.

Hydroxyaluminosilicate colloid-borne actinides

The hydroxyaluminosilicate colloids, which have been synthesized from HAS-polysilicic acid and from HAS-monosilicic acid, have a completely different behaviour in the interaction with actinides, e.g. different incorporation patterns as well as incorporation kinetics for Am and Th, different colloid-borne Cm species as identified by TRLFS, and different stability characteristics [1]. The fact that the chemical affinity of the Al^{3+} ion towards complexation is preferentially marked with polysilicic acid [18] implies that the formation of aluminosilicate colloids may also be different, depending whether monosilicic or polysilicic acid is involved as an initial reactant. Formation of the HAS colloid-borne

actinide (An) species is favored by increasing pH and concentration of Si and Al. Accordingly, maximum association of actinides with the HAS colloids is found at neutral or high pH for HAS colloids generated from polysilicic acid. In case of trivalent actinides, as identified by TRLFS [21], the "complete incorporated Cm", Cm-HAS(III) species, forms during a co-nucleation process and prevails under the experimental conditions. The actinides affinity to co-nucleate with HAS colloids formed from polysilicic acid is higher for the more hydrolyzed actinides in the order An(IV) = An(VI) >An(III), whereas Np(V) does not take part in the process of the HAS colloids formation in its nonhydrolysis pH range. Within the HAS colloids, the binding of Am(III), as that of Al(III) is directed towards the silanol groups, though with lower affinity as for Al(III). Am(III) discrimination at the co-nucleation with polysilicic acid appears to be correlated with its lower tendency towards hydrolysis as compared to that of Al(III). Whereas no kinetic effect is observed in the case of Am, the incorporation kinetics of Th and U into the HAS – polysilicic acid colloids, which is slow at low pH, resembles the polymerization kinetics of the monosilicic acid. From these observed facts, it appears evident that the essential condition for the co-nucleation is the hydrolysis of the involved elements. The process is controlled by the pH and the characteristics of the element. However, these parameters also influence the self nucleation (polymerization) reaction of individual hydrolyzed species. In order that the co-nucleation process is favorable, it is important that the rates of the nucleation reactions of the individual elements are slightly different. When HAS colloid-borne actinides are generated by titration of acidic solutions containing aluminium and actinide ions with basic monosilicic acid solution undersaturated with respect to amorphous silica in the pH range 4 – 9, the reaction starts with the Al hydrolysis, its dimerization and co-nucleation with $Si(OH)_4$ and the An hydrolyzed species. In this case the formation of a surface takes place by a self-catalyzing mechanism, which is a process with slow kinetics. Thus the HAS colloids are less stable and less efficient to incorporate the actinides. In the case of HAS formed from polysilicic acid the silicic acid concentration attains during the reaction an oversaturation level, $Si(OH)_4$ undergoes polymerization generating a surface. This preformed surface catalyzes the co-nucleation reaction with Al and An hydrolyzed species. At this stage we could distinguish different incorporation mechanisms of actinides depending on their oxidation state. Am(III), just like Al(III) binds to the silanol groups of the polysilicic acid and at pH = 8 the well-known high affinity of polysilicic acid towards $Al(OH)_3$ and $Al(OH)_4^-$ species allows the complete incorporation of Am(III) species into the HAS colloids. Th(IV) and U(VI) hydrolyzed species

copolymerizes with polysilicic acid, and further binds via oxo-bridiging to the hydrolyzed Al species with the generation of the actinide – HAS pseudocolloids. The non-hydrolyzed Np(V) does not take part in the conucleation process in the pH range ≤ 9.
HAS colloids generated from monosilicic acid appear to have lower capacity to hold Am(Eu), U and even much lower for Th, in the latter case a 100 times less as compared to the HAS generated from polysilicic acid. For both HAS-monosilicic or polysilicic acid colloids the capacity of incorporating Am and Th increases generally with increasing pH [2].

3.4 Stability of Hydroxyaluminosilicate (HAS) colloids and colloid-borne actinides

As already discussed in chapter 3.2, a condition sine qua non for the colloidal actinide migration is the irreversible binding of actinides to stable colloids. In the case of HAS pseudocolloids of actinides, not only the irreversibility of the actinide/HAS binding is questioned, but also the irreversibility of the aluminosilicate bindings itself. Once generated and stabilized in water, the colloids are able to be transported along the water pathway. By definition colloids are metastable and the question is: can those colloids survive over a long time period during migration? In the following, we test the resistance of HAS colloids and colloid-borne actinides relative to changes which are likely to occur in natural open systems, namely variations in pH, temperature, occurrence of ligands such as EDTA and humic acids, presence of cations, and the silicon and aluminium concentration gradient.

EDTA resistance

As mentioned above (see section 3.2), EDTA is a well known chelating agent which forms very stable complexes with most metals and potentially competes with Si-ligands for binding actinides or Al(III) and may promote their release from HAS colloids through formation of soluble EDTA complexes. The EDTA resistance of the Al-O-Si binding is analyzed in the following not only for HAS generated from polysilicic acid but also for HAS generated from monosilicic acid. For this purpose HAS solutions are prepared in absence of actinides at pH 5, 7, and 9. After a conditioning time varying between 3 hours and 260 days, the HAS solutions are brought into contact with EDTA at a final concentration of 10^{-3} M. At different time intervals, the soluble Al is determined in the solution remaining after removal of precipitate and colloids, as described in the appendix.

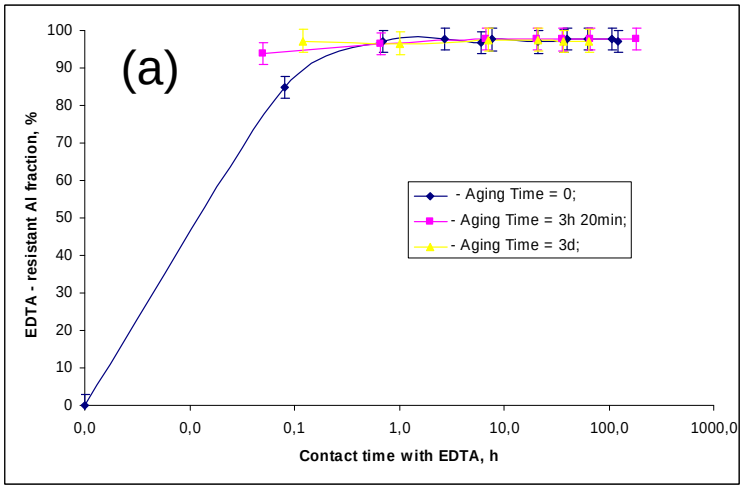

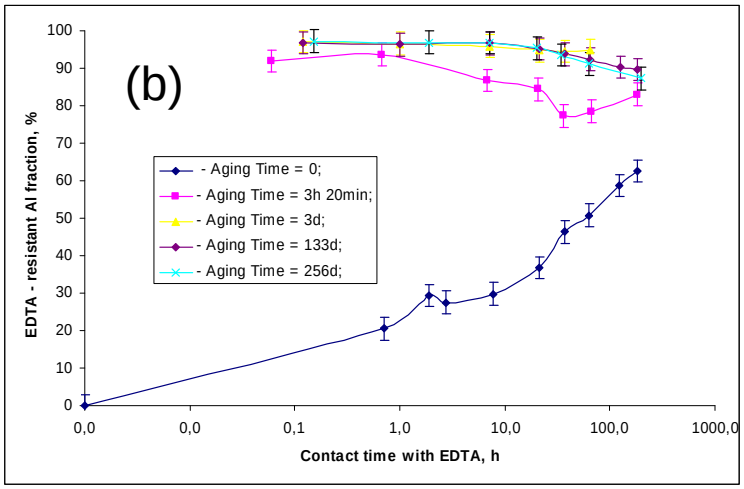

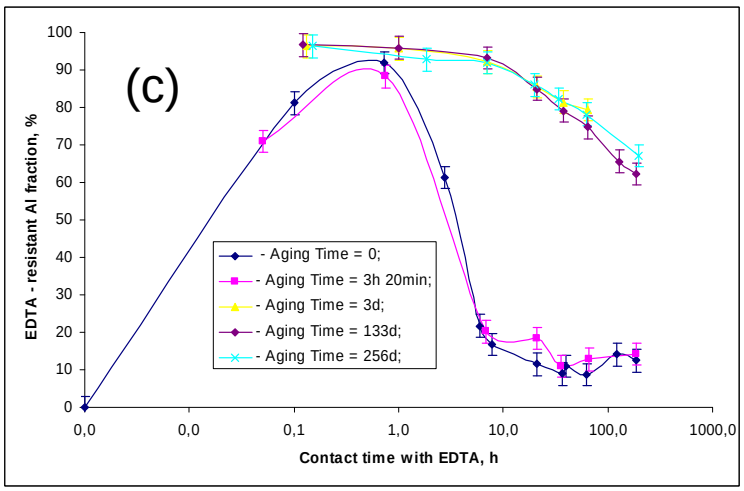

Figure 11 The EDTA-resistant Al fraction within the HAS colloids generated from polysilicic acid at pH 9 (a), 7 (b) and 5 (c) as a function of contact time with 1.3x10-3 mol·l-1 EDTA. The order of reactant addition at sample preparation and aging time is indicated in the legend. Time zero marks the moment of addition of EDTA or silicic acid.

The EDTA resistant Al is obtained by subtracting the concentration of soluble Al from the Al concentration initially introduced in the sample. A separate experiment is carried out under identical concentration conditions but with changed sequence of component addition, namely: Al solution is first contacted with EDTA followed by addition of Si after 3 hours conditioning time (marked as Aging time = zero). Figure 11 illustrates the results for the EDTA-resistant Al fraction (Al nonsoluble, %) as a function of EDTA contact time.

For the HAS generated from polysilicic acid at pH 9 (Figure 11a), the colloid-borne Al appears to be EDTA resistant even for only 3 hours aged aluminosilicate solutions (the pink curve). At this pH we expect that EDTA does not interact with polysilicic acid, both molecules being negatively charged. It means that at pH 9 polysilicic acid is a stronger complexing ligand. At pH 5 (Figure 11c), the colloid-borne Al aged for 3 hours is less stable. After an initial increase of the stable Al fraction, most Al appears to be complexed by EDTA and transferred to the solution within 10 – 20 days. A marginal

amount of about 14 % colloid-borne Al can be still observed after 7 months. This behavior might be explained by an initial rapid sorption process of the Al-EDTA complex onto the surface of the polysilicic acid as at pH 5 the EDTA is not fully deprotonated and retains residual protons which may bind to the polysilicic acid surface.

During re-equilibration, desorption of the Al-EDTA complex occurs and Al is released again into the solution. However, the colloid-borne Al aged for several days appears more EDTA – resistant: a marginal amount of about 60 % colloid-borne Al can still be observed after 7 months contact time with EDTA at pH 5. At pH 7 (Figure 11b), 90 % of the colloid-borne Al aged for 3 hours or several days remains stable in presence of 10^{-3} M EDTA within the observation time.

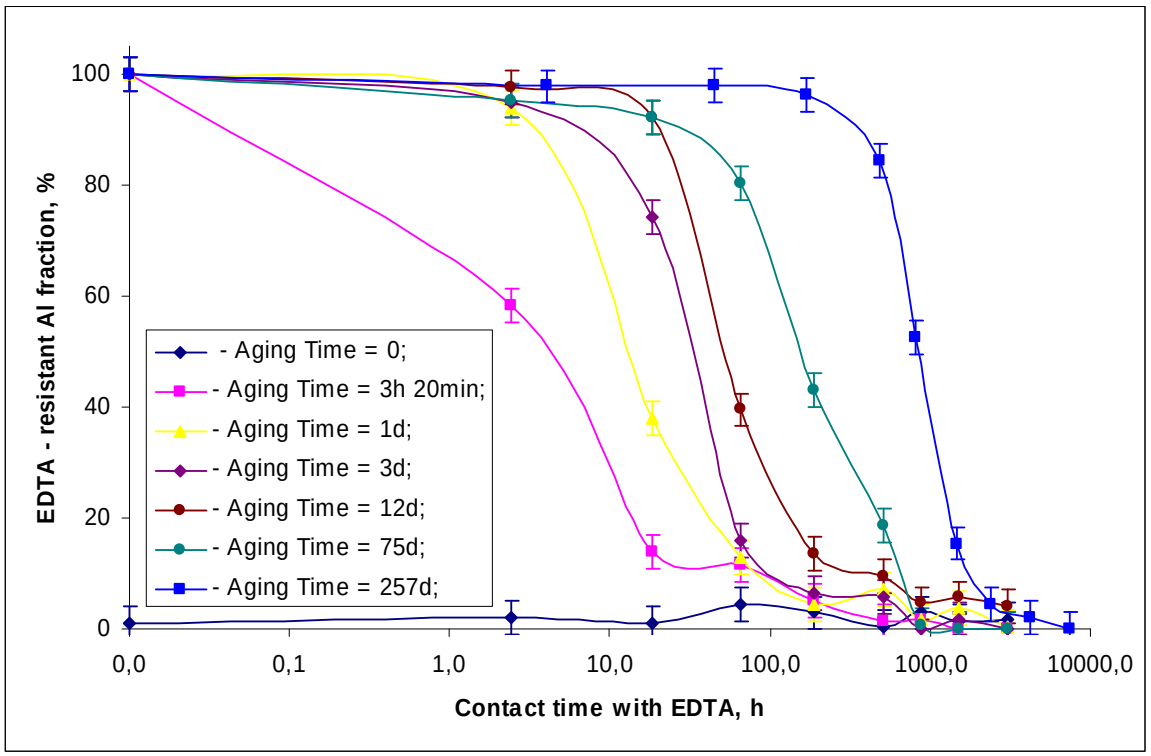

Figure 12 The EDTA-resistant Al fraction within the HAS colloids generated from monosilicic acid at pH 7 as a function of contact time with 1.3×10^{-3} mol·l^{-1} EDTA. The aging time at 23ºC is indicated in the legend. Time zero marks the moment of addition of EDTA or silicic acid.

A separate experiment series is additionally carried out under the same conditions but with a changed sequence of component addition in order to test whether reaction equilibrium is achieved within the time of observation. The results are indicated in Figure 11 by the dark blue curves. It seems that at least several years are required to achieve the steady state conditions. As can be seen, the EDTA stability of the Al-O-Si binding within the colloids is higher with increasing pH and at prolonged conditioning time (aging) of the system. At

slightly alkaline pH polysilicic acid is a stronger complexing ligand and can displace the EDTA in the Al coordination sphere. This fact is not observed for the aluminosilicate solutions generated from monosilicic acid (see Figure 12) as Al remains in solution complexed with EDTA.

In case that HAS is formed from monosilicic acid (see Figure 12) the Al-O-Si binding becomes more EDTA vulnerable. The effect is again pH and time dependent as expected. The increased Al stability with sample ageing can be due to the changes in the binding state of Al within the HAS. Also in some instances, aluminosilicates may crystallize in the amorphous mass after aging, especially if components are present in suitable stoichiometric proportions. One should also take into account possible changes in the geometry (aggregation) of the solid phase resulting in a smaller surface area in contact with the solution and, consequently lower Al dissolution rates.

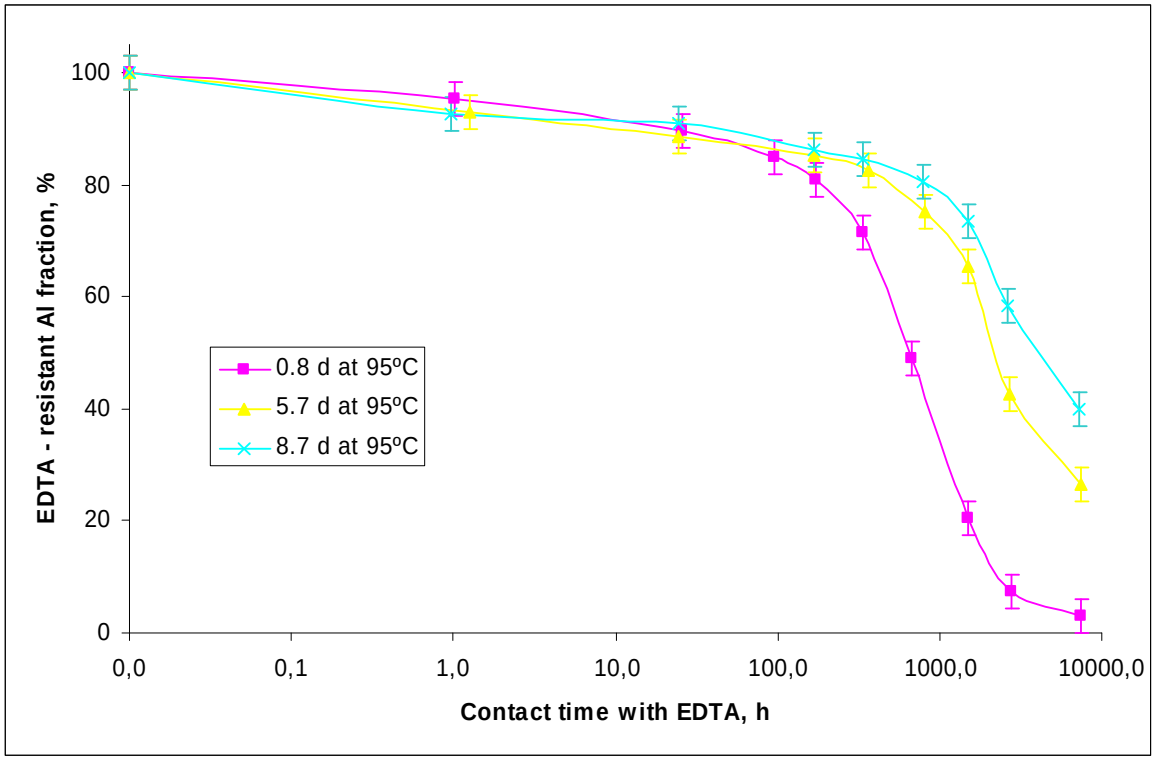

Figure 13 The EDTA-resistant Al fraction within the HAS colloids generated from monosilicic acid at pH 7 as a function of contact time with $1.3x10^{-3}$ mol·l^{-1} EDTA. The aging time at 95ºC is indicated in the legend.

The next experiment intends to study the role of temperature on the Al-O-Si binding strength that is relevant to geothermal and hydrothermal systems like high-level nuclear waste repositories. The results presented in Figure 13 show that enhancing the sample temperature from 23ºC to 95ºC further stabilizes the Al-O-Si bindings. As suggested by the

Arrhenius equation: $\ln(k2/k1) = E_a/R(1/T1-1/T2)$, where k1, k2 are the rate constants at temperatures T1 and T2, respectively, E_a is the activation energy (~ 80 $kJ \cdot mol^{-1}$) and R is the gas constant, the temperature effect might be achieved by increasing the aging time of the mother solution. In relation to this aspect, we can translate temperature into time: 19 hours at 95ºC becomes 470 days at 23ºC, 5.7 days at 95ºC becomes 9 years at 23ºC and 8.7 days are equivalent with 14 years at 23ºC. Underlining assumption is, of course, that the temperature has no other effect than to influence the kinetics.

In order to get a relative assessment of the actinide-colloid binding strength under the condition of maximum formation of colloid-borne actinides, a ligand competition experiment is further carried out, with the aid of EDTA as competitor for the HAS colloids.

Table 5 Distribution of Th activity fraction (%) normalized to the input activity between the precipitate, colloids and solution as a function of EDTA contact time. Samples with initial composition of 8.7x10-6 M Th in 0.03 M NaCl at pH 5, 7 and 9 are conditioned for 1 day before addition of EDTA with final concentration $1x10^{-3}$ M. Time 0 marks the moment before EDTA addition.

Time, days	pH = 5			pH = 7			pH = 9		
	ppt, %	coll, %	ion, %	ppt, %	coll, %	ion, %	ppt, %	coll, %	ion, %
0	99.4	0.5	0.1	99.8	0.1	0.1	99.9	0.0	0.1
0.14	33.7	0.2	66.1	9.0	5.0	86.0	65.3	19.8	14.9
1.91	15.4	0.5	84.2	4.8	2.4	92.8	3.9	2.8	93.3
5.94	12.8	1.5	85.8	5.0	2.5	92.4	2.6	1.2	96.2
9.95	12.6	0.5	87.0	5.1	1.8	93.1	2.4	3.2	94.4
19.9	10.9	1.5	87.5	4.2	3.6	92.3	2.1	2.7	95.1
40.91	9.5	0.7	89.8	4.4	1.0	94.6	2.5	0.6	96.8

Table 6 U activity fraction (%) normalized to the input activity in the precipitate, colloids and solution as a function of EDTA contact time. Samples with initial composition of $8.7x10^{-6}$ M U in 0.03 M NaCl at pH 5 and 9 are conditioned for 1 day before addition of EDTA with final concentration $1x10^{-3}$ M. Time 0 marks the moment before EDTA addition.

Time, days	pH = 5			pH = 9		
	ppt, %	coll, %	ion, %	ppt, %	coll, %	ion, %
0	16.2	27.6	56.1	5.3	63.9	30.8
0.08	2.2	3.9	93.8	3.2	26.9	69.9
1.08	2.8	3.1	94.1	3.3	8.2	88.5
5	3.1	1.6	95.3	14.9	6.1	78.9
9	4.3	0.2	95.6	20.7	2.8	76.5
15.06	4.3	0.8	94.9	23.6	7.8	68.5

41.2	4.2	0.7	95.1	25.8	5.1	69.1

The desorption experiments are carried out on 3 series of samples corresponding to Am(III), Th(IV) and U(VI). Each series of samples consists of 8.6×10^{-7} M actinide and 10^{-2} M Si / 10^{-4} M Al corresponding to the synthesis of HAS from polysilicic acid at pH 7 and 9. The samples are conditioned for 1 day, long enough to ensure the formation of maximum colloid-borne fractions of Th(IV) and U(VI) which have been shown to have fast kinetics of incorporation at these pH and Si concentration. In case of trivalent actinides, as outlined in section 3.3 the "complete incorporated Cm", (Cm-HAS(III) species), forms during a co-nucleation process and prevails under the experimental conditions. After a 1 day conditioning time with actinides, EDTA is added at a final concentration of 1×10^{-3} M. The partition of the actinide activity fraction in the three phases is monitored before EDTA addition and at different intervals thereafter. EDTA competes with the HAS for binding the actinides and promotes their desorption from the HAS colloids by formation of complexes in solution. The experimental EDTA concentration, one order of magnitude higher than that of Al, is in larger excess to the actinide ensuring its complete complexation. First, blank experiments are performed by adding EDTA to solutions of pH 5, 7, and 9 containing only the actinide, because once in solution, the actinides tend to hydrolyze with formation of hydroxo complexes and hydroxide solid phases, the reaction will compete with the complexation by EDTA.

Table 7 Am activity fraction (%) normalized to the input activity, in the precipitate, colloids and solution as a function of EDTA contact time. The samples with initial composition (8.7×10^{-6} M Eu(Am), 1.5×10^{-4} M Al and 1.3×10^{-2} M Si, at pH 7 and 9) are conditioned for 1 day before addition of EDTA (1×10^{-3} M). Time 0 marks the moment before EDTA addition.

Time, days	pH = 5			pH = 9		
	ppt, %	coll, %	ion, %	ppt, %	coll, %	ion, %
0	8.6	90.4	1.1	2.5	95.6	1.9
0.14	7.5	36.6	55.9	3.1	63.4	33.5
1.14	7.2	15.7	77.1	3.4	32.0	64.6
1.89	7.4	11.0	81.6	3.1	22.9	74.1
2.9	7.9	8.4	83.8	4.1	15.3	80.6
5.98	8.9	5.3	85.9	2.9	11.2	86.0
9.88	9.0	3.9	87.1	2.5	7.3	90.2
16.08	8.2	3.3	88.5	2.8	4.6	92.6
22.9	8.2	2.8	89.0	2.6	3.7	93.7
29.89	7.8	2.4	89.8	2.6	2.7	94.7
43.93	8.6	2.0	89.4	2.9	2.2	94.9

112	8.2	2.5	89.3	2.5	3.7	93.8

The results show that the activity fraction is transferred completely to the solution and the precipitation of hydrolysis species is not attained. Selected results are given in Tables 5 and 6. Tables 7, 8, and 9 give the results on the actinide partition between the three phases in presence of HAS as a function of EDTA contact time.

Table 8 Th activity fraction (%) normalized to the input activity, in the precipitate, colloids and solution as a function of EDTA contact time. The samples with initial composition ($8.7x10^{-6}$ M Th, $1.5x10^{-4}$ M Al and $1.3x10^{-2}$ M Si, at pH 7 and 9) are conditioned for 1 day before addition of EDTA ($1x10^{-3}$ M). Time 0 marks the moment before EDTA addition.

Time, days	pH = 5			pH = 9		
	ppt, %	coll, %	ion, %	ppt, %	coll, %	ion, %
0	2.5	80.1	17.4	0.3	58.0	41.7
0.16	4.5	80.4	15.1	0.6	59.9	39.5
0.95	4.3	87.0	8.7	0.4	61.4	38.3
1.95	5.3	88.7	6.1	1.0	61.6	37.4
4.98	4.4	91.6	4.1	1.2	61.3	37.5
8.94	3.5	93.2	3.3	0.5	62.2	37.4
15.14	3.4	93.4	3.2	0.8	64.6	34.6
21.95	2.8	94.2	3.0	0.3	68.2	31.5
28.94	2.9	93.7	3.4	0.4	68.6	31.0
42.99	3.0	93.3	3.7	-0.1	71.5	28.5
111	-0.6	96.5	4.1	0.5	79.9	19.6

Table 9 U activity fraction (%) normalized to the input activity, in the precipitate, colloids and solution as a function of EDTA contact time. The samples with initial composition ($8.7x10^{-6}$ M U, $1.5x10^{-4}$ M Al and $1.3x10^{-2}$ M Si, at pH 7 and 9) are conditioned for 1 day before addition of EDTA ($1x10^{-3}$ M). Time 0 marks the moment before EDTA addition.

Time, days	pH = 5			pH = 9		
	ppt, %	coll, %	ion, %	ppt, %	coll, %	ion, %
0	2.9	96.2	0.9	1.5	96.9	1.6
0.15	2.5	94.8	2.7	2.0	96.2	1.8
1.14	2.3	95.1	2.5	2.0	96.5	1.5
1.9	1.1	96.4	2.5	1.1	97.5	1.4
6	2.8	94.9	2.4	1.6	97.1	1.3
9.89	1.6	96.1	2.2	0.5	97.6	1.9
16.09	1.7	96.1	2.3	1.5	97.3	1.2
22.91	1.3	96.5	2.2	0.6	98.2	1.2
29.9	1.3	96.2	2.5	0.8	97.8	1.4
43.94	1.7	96.0	2.3	0.7	98.1	1.2
112	1.4	96.1	2.6	0.8	97.9	1.3

As can be seen, the Am activity fraction in the colloidal phase decreases rapidly upon contact with EDTA. The main part of the initially colloid-borne Am is desorbed from the colloids within 2 days contact time with EDTA at all pH. It is obvious that under the conditions ensuring the strongest An(III) binding to the HAS (i.e. incorporation of Cm(III) into the HAS colloids), the HAS colloid-borne Am is not EDTA resistant. The result is also corroborated by TRLF spectroscopy. In contrast, Th(IV) and U(VI) remain as colloid borne species in presence of EDTA over a long time span. The slow increase in the colloidal Th activity fraction observed after prolonged EDTA contact time is due to an incomplete incorporation of Th into the HAS colloids at the moment of EDTA addition.

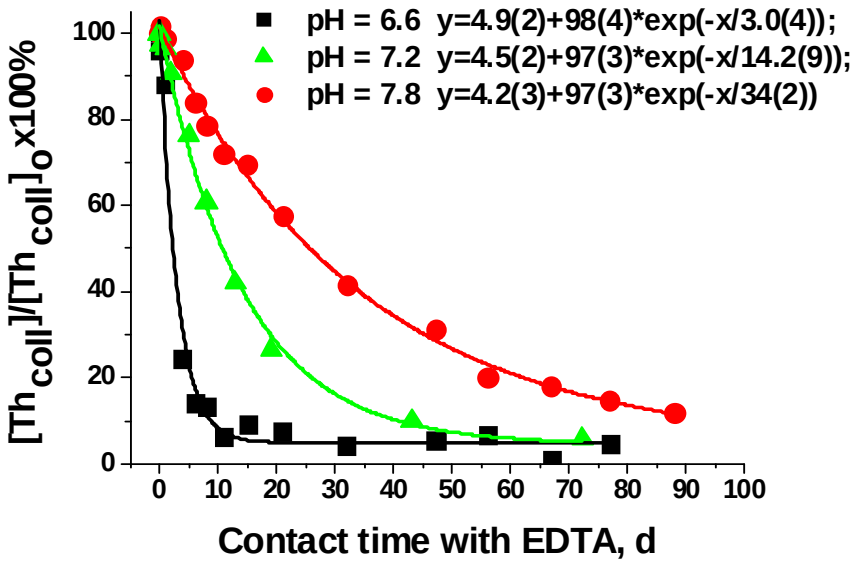

Figure 14 EDTA resistant Th fraction within the HAS colloids normalized to the initial Th concentration in the HAS colloids as a function of contact time (days) with EDTA. The HAS solutions are generated from and monosilicic acid and consist of 1.4×10^{-3} M Si / 1.3×10^{-5} M Al / 5×10^{-8} M Th. Time 0 marks the moment of addition of EDTA.

The kinetics of dissociation of Am and Th from HAS colloids generated from monosilicic acid is studied further. During the experiment the pH is maintained constant at 6.6, 7.2, and 7.8 with aid of 0.01 M MOPS buffer. The initial samples are prepared with 5 x 10^{-8} mol·l^{-1} Am or Th, 1.4×10^{-3} mol·l^{-1} Si, 1.3×10^{-5} mol·l^{-1} Al. The desorption experiment is conducted by addition of a small volume of EDTA to the water/aluminosilicate system containing 35 days aged Am-HAS or Th-HAS pseudocolloids to give a final concentration of 10^{-4} mol·l^{-1} EDTA. Small aliquots of the aqueous suspension are removed and filtered using two different types of membrane filters as described above (see section 2) immediately prior to

the addition of EDTA (t = 0) and at intervals thereafter to determine dissolved and colloidal actinide fractions as a function of time. In each filtrate the actinide concentration is determined by liquid scintillation counting. Figures 14 and 15 illustrate selected results for the fraction of actinide bound to the HAS colloids as a function of time at different pH values.

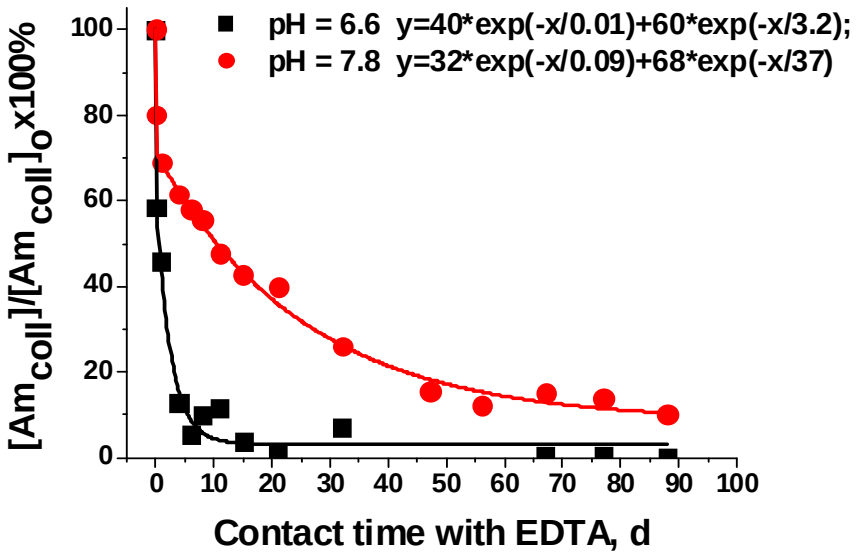

Figure 15 EDTA resistant Am fraction within the HAS colloids normalized to the initial Am concentration in the HAS colloids as a function of contact time (days) with EDTA. The HAS solutions are generated from and monosilicic acid and consist of 1.4×10^{-3} M Si / 1.3×10^{-5} M Al / 5×10^{-8} M Am. Time 0 marks the moment of addition of EDTA.

As can be appreciated from the picture, the colloid-borne actinides are not EDTA resistant irrespective of pH. The desorption kinetics is clearly hindered and the rate of the Th and Am dissociation from HAS colloids decreases with increasing pH. It gives a direct consequence of the proton-dependent dissolution. All Th-kinetic dissociation curves are fitted by a mono-exponential function and at least two different Am-HAS species, showing fast and slow dissociation kinetics, are necessary to fit the experimental results. Also, as evidenced by TRLFS and discussed in section 3.3, different Cm-colloid-borne species with different Cm-HAS affinity form, depending on the pH of the solution. It is conceivable that such species show different desorption kinetics. The difference in the kinetic curves observed in Figures 14 and 15 can be explained by a first-order process in $[H^+]$. When pH increased from 6.6 to 7.8, the time required to achieve 99 % of equilibrium increased from 1 hour to 8 hours for the first species Am-HAS(I) and from 11 days to 130 days for the second species Am-HAS(II). The Am-HAS(II) species is the prevailing colloidal species at both pH values. Its fraction increases with increasing pH. Th desorbs from HAS colloids

with a dissociation time constant of the same order of magnitude as for the Am-HAS(II) species. When pH increased from 6.6 to 7.8, the time required to achieve 99 % equilibrium increased from 13 days to 130 days. The study of the dissociation kinetics of actinides from HAS colloids by the ligand-competition method with EDTA provides important insights into the nature of metal binding in this system. Th(IV) appears to have a higher affinity to HAS colloids in comparison with Am(III) according to the order of actinide valence state adsorption to environmental colloids.

Dilution experiment

The next experiment intends to study the stability of HAS colloids and the role of kinetics at the formation of the HAS colloids. For this purpose HAS solutions are prepared at pH 9 by titration a 0.03 $mol \cdot l^{-1}$ HCl acidic solution, containing $2x10^{-4}$ $mol \cdot l^{-1}$ aluminium chloride, with a 0.03 $mol \cdot l^{-1}$ NaOH solution, containing $2x10^{-2}$ $mol \cdot l^{-1}$ sodium silicate. The resulting suspensions are aged for different time periods in a plastic bottle and then diluted in Milli-Q water in proportion 1:100. The stability of HAS colloids is monitored at room temperatures between 20 and 23ºC by determining the monomeric silica concentration at different time intervals. The concentration of silica is determined spectroscopically by the molybdenum test. Results of these tests are shown in Figure 16, which shows that stable HAS colloids might exist in water solutions even at quite low silica concentration at circum-neutral pH, namely 10^{-4} $mol \cdot l^{-1}$ (solubility of silica is circa $2x10^{-3}$ $mol \cdot l^{-1}$). Dissolution of silica initiated after 806 days is as rapid as for the HAS colloids heated to 80ºC for 5 days, indicating that temperature accelerates the aging process with an Arrhenius activation energy of approximately 77 $kJ \cdot mol^{-1}$ (18 $Kcal \cdot mol^{-1}$).

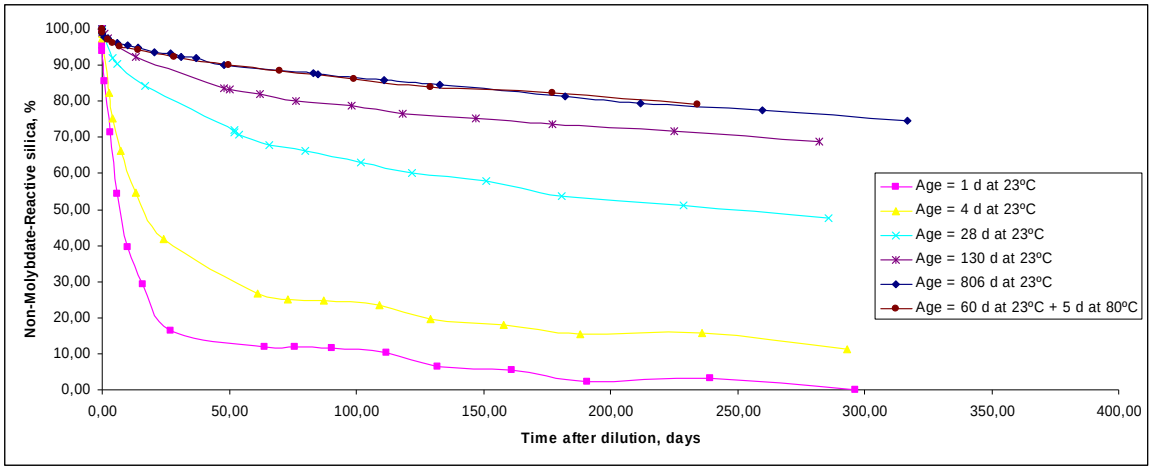

Figure 16 Dissolution of the HAS colloids generated from polysilicic acid in water at pH 7.3. The aging time at room and higher temperature is indicated in the legend. [Al] = 10^{-6} mol·l^{-1}; [Si] = 10^{-4} mol·l^{-1}.

The initial rates of dissolution are several times greater than the rates after one or more days depending on the pre-equilibration time before dilution. A similarly rapid time-scale was previously observed in the early portions of EDTA-induced dissolution experiments (see above). In a second series of experiments the influence of pH on the dissolution kinetics is investigated. The pH values are adjusted by the addition of small amounts of hydrochloric acid or sodium hydroxide, thus avoiding the influence of foreign ions from the application of buffers. Our investigations show that the dissolution rate constants of the HAS colloids decrease with decreasing pH value of the solution and at prolonged conditionings time of the suspension. This behaviour is in agreement with expectation.

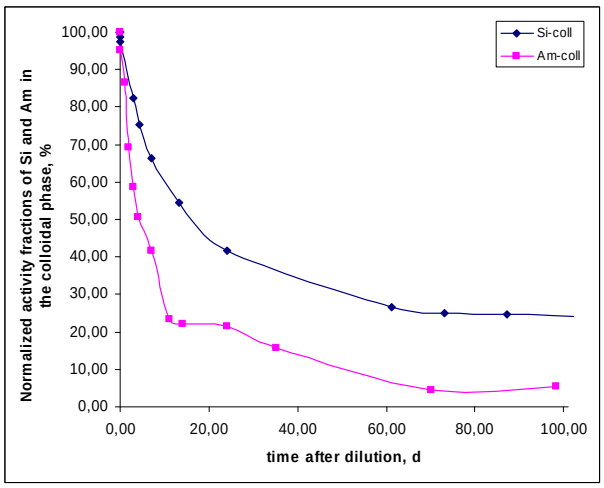

Figure 17 Dissolution of the HAS and ^{241}Am-labelled HAS colloids in deionized water at pH 7.3. The HAS colloids are generated from polysilicic acid and aged for 4 days at room temperature. [Al] = 10^{-6} mol·l^{-1}, [Si] = 10^{-4} mol·l^{-1}, [Am] = 4x10^{-8} mol·l^{-1}.

In our previous work [1] it was shown that for pH > 6 trivalent colloid-borne actinides formed by coprecipitation with polysilicic acid are incorporated into the structure of aluminosilicates colloids. That species already prevails at pH 7 (more than 60 %) and remains stable with time. 10^{-2} M silicon and 10^{-4} M aluminium concentrations are, however, not really relevant for the far-field repository conditions. It must be mentioned, that aluminium concentration in waters varies between 3.7x10^{-8} mol/l and 1.4x10^{-4} mol/l and silicon concentration shows smaller differences, from 6.2x10^{-5}

mol/l to $4.5x10^{-4}$ mol/l. On the other hand, the silica might be dissolved in geothermal and hydrothermal systems like high-level nuclear waste repositories. Over the designed lifetimes of the repository, large quantities of silica might be dissolved and transported from the rocks overlying the repository zone undergoing dilution in water [31]. While colloid transport is in itself not of primary interest, ^{241}Am-labelled HAS colloids are used for the next dilution experiment that consists of the analysis of the stability of the HAS colloid-borne actinides at changing conditions, which are likely to occur in an open natural aquatic system.

The colloidal solution is prepared by titrating an acidic solution, containing $2x10^{-4}$ mol/l Al(III) and $8x10^{-6}$ mol/l Am(III) metal ions, with a basic solution, containing $2x10^{-2}$ mol/l silicate ions, to a pH 9. The resulting suspension is aged for four days at room temperature in a plastic bottle and then diluted in Milli-Q water in proportion 1:100. After the required dilution, the pH is shifted to 7.3 and the americium concentration becomes of the order of $4x10^{-8}$ M with at least 86 % associated initially with HAS colloids. The stability of HAS colloids is monitored at temperatures between 20 and 23ºC by determining the monomeric silica concentration and colloid-borne Am fraction versus time. The concentration of silica in the filtered solution is determined by the molybdenum test (see section 2.4). Figure 17 shows that as the silica concentration is reduced by dilution, the high-molecular weight silicic acid concentration decreases. The dissolution reaction rate is calculated for each experiment by measuring the slope of the concentration-time plot during the early stage of the experimental run. The initial rate of silica dissolution is circa 6 % per day and the initial vanishing rate of Am from HAS colloids is circa 12 % per day. The dissolution rates become comparable between 11 and 100 days. The experiment shows that fresh HAS colloids do not demonstrate high stability towards dissolution in water. Americium disappears from HAS colloids even faster and is found to be sorbed on the vessel wall by the end of the experiment.

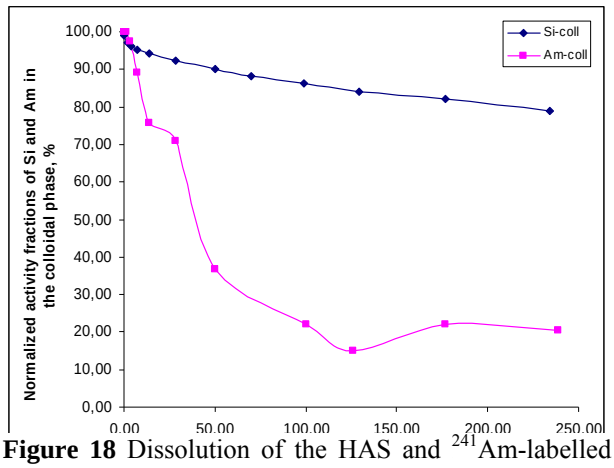

Figure 18 Dissolution of the HAS and ^{241}Am-labelled HAS colloids in deionized water at pH 7.3. The HAS colloids are generated from polysilicic acid and aged for 58 days at room temperature and 5 days at 80ºC. [Al] = 10^{-6} mol·l^{-1}, [Si] = 10^{-4} mol·l^{-1}, [Am] = $4x10^{-8}$ mol·l^{-1}

In the next experiment the HAS colloids with and without ^{241}Am are prepared again at pH 9, aged for 31 days and heated at 80ºC for 5 day to accelerate the aging process. The heating procedure reduces the association of americium with the HAS colloids to 51 %. The resulting

suspensions are aged again for 27 days at room temperature and then diluted in Milli-Q water in proportion 1:100, and the time dependence of concentrations of the low-molecular weight silicic acid and americium are traced again. The graph of the dissolution is shown in Figure 18. The results illustrate that increasing the aging time and/or enhancing the sample temperature from 23ºC to 80ºC stabilize the HAS colloids and the Am – HAS colloid binding. The initial rate of silica dissolution is circa 0.4 % per day and the initial vanishing rate of Am from HAS colloids is circa 1.7 % per day. A marginal amount of about 20 % colloid-borne Am is still observed even after 8 months.

In addition, for pH 7, the effect of HA and metal ions (separately and complementary) on the HAS colloidal solution stability is tested. The colloidal solutions are prepared by titrating an acidic solution, containing varying concentrations of metal ions (Al(III), Eu(III), Am(III), Th(IV)), with a basic solution, containing silicate ions, to a pH~9. The resulting suspensions are aged for four days and then diluted in Milli-Q water in proportion 1 to 100. Aliquots of each sample are taken to measure the monomeric silica concentration to evaluate the stability of HAS colloids as a function of time.

Figure 19 illustrates the influence of Eu(III) on the dissolution kinetics of silica and HAS colloids. As can be seen, the molybdate-reactive orthosilicic acid concentration increases rapidly at higher europium content due to formation of soluble silicate complexes. The same effect is observed for thorium and uranium ions. A relatively high concentration of salts such as sodium chloride is required to promote the dissolution of silica. Aluminium ions produce the opposite effect.

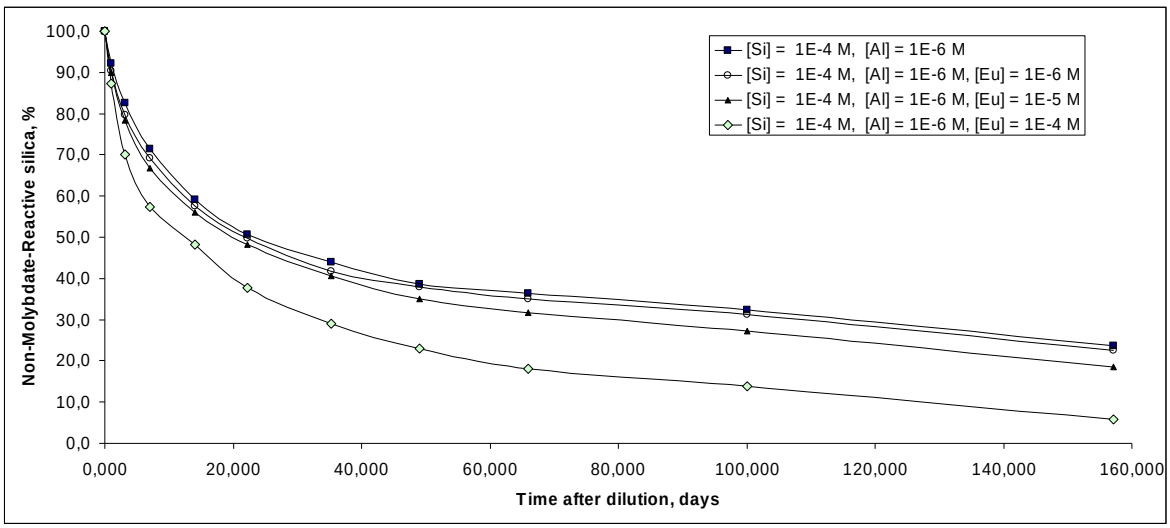

Figure 19 Dissolution of the HAS colloids in deionized water at pH 7.3. The HAS colloids are generated from polysilicic acid in presence of varied Eu concentrations, aged for 4 days at room temperature and then diluted in Milli-Q water in proportion 1 to 100.

Figure 20 demonstrates the very strong inhibition of the depolymerisation of colloidal silica by hydrolyzed aluminium at pH 6.6 and 7.8 in 0.01 M MOPS buffer solution. Surprisingly, the shaking is found do not affect significantly the rate of solution of the colloid silica. But higher temperature and pH accelerate silica dissolution as expected.

As organic coatings may stabilize colloids [32], the influence of HA on the dissolution rate of HAS colloids is studied further. In another sample series, small aliquots of HA stock solution are introduced to colloidal HAS solution immediately after its dilution to give a final HA concentration varying from 0 to 10 mg/l. The results show that HA influence silica dissolution rates indirectly, primarily through their complexation with aluminium and other metal ions. Humic acid competes with the colloidal silica for aluminium ions and counteracts the effect of Al in decreasing the dissolution rate of HAS colloids. In this case HA accelerates dissolution. In a similar way HA decreases the concentration and activity of inorganic Eu and Th species and counteracts their effect in increasing the dissolution rate of HAS and silica colloids. Thus in this case HA inhibit dissolution.

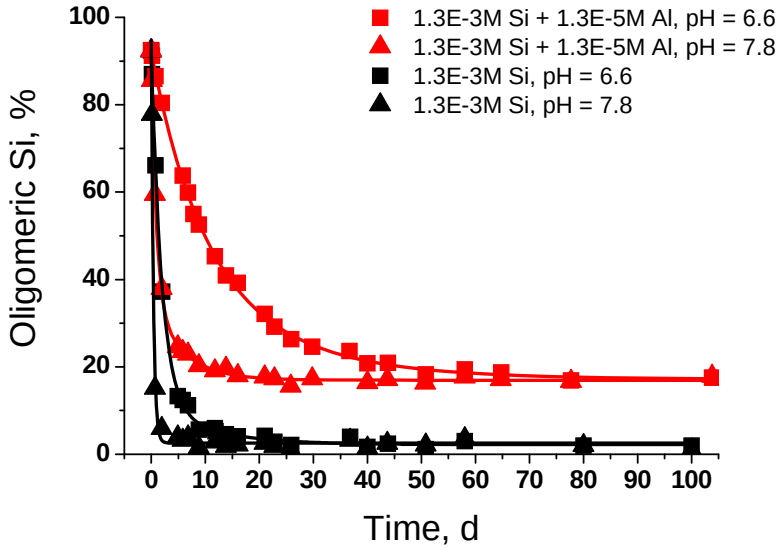

Figure 20 Dissolution of the HAS colloids in deionized water at pH 6.6 and 7.8. The HAS and silica colloids are generated from polysilicic acid at room temperature and then diluted in Milli-Q water in proportion 1 to 30.

Table 10 ^{32}Si activity fraction (%) normalized to the initial activity in the precipitate, colloids and solution as a function of pH, Eu, Si, HA and Al concentration. Results represent values obtained after 35 d sample conditioning time.

pH	*c(Eu), M*	*c(HA), ppm*	*c(Si), M*	*c(Al), M*	*ppt(Si), %*	*col(Si), %*	*ion(Si), %*
6.6	-	6.0	1.0E-03	-	1.9	1.8	96.3
7.8	-	6.0	1.0E-03	-	0.4	2.9	96.7

6.6	-	-	1.0E-03	1.0E-04	9.2	0.7	90.1
7.8	-	-	1.0E-03	1.0E-04	5.7	7.6	86.8
6.6	-	6.0	1.0E-03	1.0E-04	7.7	1.4	90.9
7.8	-	6.0	1.0E-03	1.0E-04	7.8	7.8	84.3
6.6	1.0E-05	-	1.0E-03	-	3.0	0.2	96.8
7.8	1.0E-05	-	1.0E-03	-	2.5	0.3	97.2
6.6	1.0E-05	6.0	1.0E-03	-	1.0	2.1	96.9
7.8	1.0E-05	6.0	1.0E-03	-	0.1	2.6	97.3
7.8	-	6.0	1.0E-05	-	1.2	0.9	97.9
7.8	-	-	1.0E-05	1.0E-05	3.3	2.0	94.7
7.8	-	6.0	1.0E-05	1.0E-05	0.9	2.8	96.3
7.8	1.0E-05	-	1.0E-05	-	3.7	0.2	96.0
7.8	1.0E-05	6.0	1.0E-05	-	2.4	1.2	96.4

Table 10 shows ^{32}Si distribution between the precipitate, colloid and solution after 35 days conditioning time of monosilicic acid and / or humic acid, and / or Eu / Al ions. There is no evidence that coatings of amorphous hydroxyaluminosilicate colloids or/and formation of mixed HAS-humic colloid species occurs under the present experimental conditions. This result is in agreement with the experimental results in [33].

3.5 Complexation of Al(III) and actinide(III)/(IV)/(VI) with silicic and humic acids

The study is continued for investigating the behaviour of Al and the actinides, either Am, Th, or U, in the mixed system humic acid-aluminosilicate. Thus, the actinides may undergo complexation with humate colloids, conucleate with silicic acid with formation of An-HAS pseudocolloids, and interact with both HAS and HA with formation of mixed HAS-humic colloidal species or a mixture of An-HAS and An-humic colloids. The formation of colloid-borne An in the presence of both HAS and humic acid (^{14}C-HA) is examined within the neutral pH range 6.6 to 7.8. The pH range is chosen to follow the low solubility regions of $Al(OH)_3$ and aluminosilicate minerals in which the HAS colloid formation is not pronounced due to precipitation [30] and thus the eventual influence of HA on the colloid formation becomes visible. HAS solutions are prepared from both undersaturated and oversaturated silica to observe colloid formation from both monosilicic and polysilicic acid, respectively. Based on the results from section 3.1, humic acid concentration is kept constant at 6.5 mg/l which appeared to be appropriate to appraise the humic acid effect. Trace amounts of actinides are used in the experiment: [^{241}Am]: $5x10^{-8}$ M, [^{234}Th + ^{232}Th]: $5x10^{-8}$ M and [^{233}U]: $8x10^{-7}$ M. A parameter screening experiment is carried out to characterize the conditions for formation of colloid-borne actinides in presence of both HAS and humic colloids for the above mentioned experimental conditions. Figure 21 gives an overview of the colloid formation for actinides interacting with the different colloid types: HAS colloids (left side of each diagram), composite of HAS and humic colloids

generated in solutions containing silicic acid, Al and HA (right side, the upper and middle contours) and humic colloids complexed with Al (right side, the lowest contours). Reference samples, containing only the actinide are also indicated (left side, lowest contours). The contours show the actinide incorporation into the colloidal phase separated by ultrafiltration. From the contour profiles for formation of HAS-colloid borne actinides (left parts of Figure 21)

one can observe that Th and U colloidal fractions are abundant for the entire pH range in presence of polysilicic acid. As outlined in section 3.3, as compared with Am, Th, and U have been shown to have higher affinity towards polysilicic acid. However, even in this case, Al concentration of 10^{-3} M destabilizes the HAS colloids and the actinides precipitate.

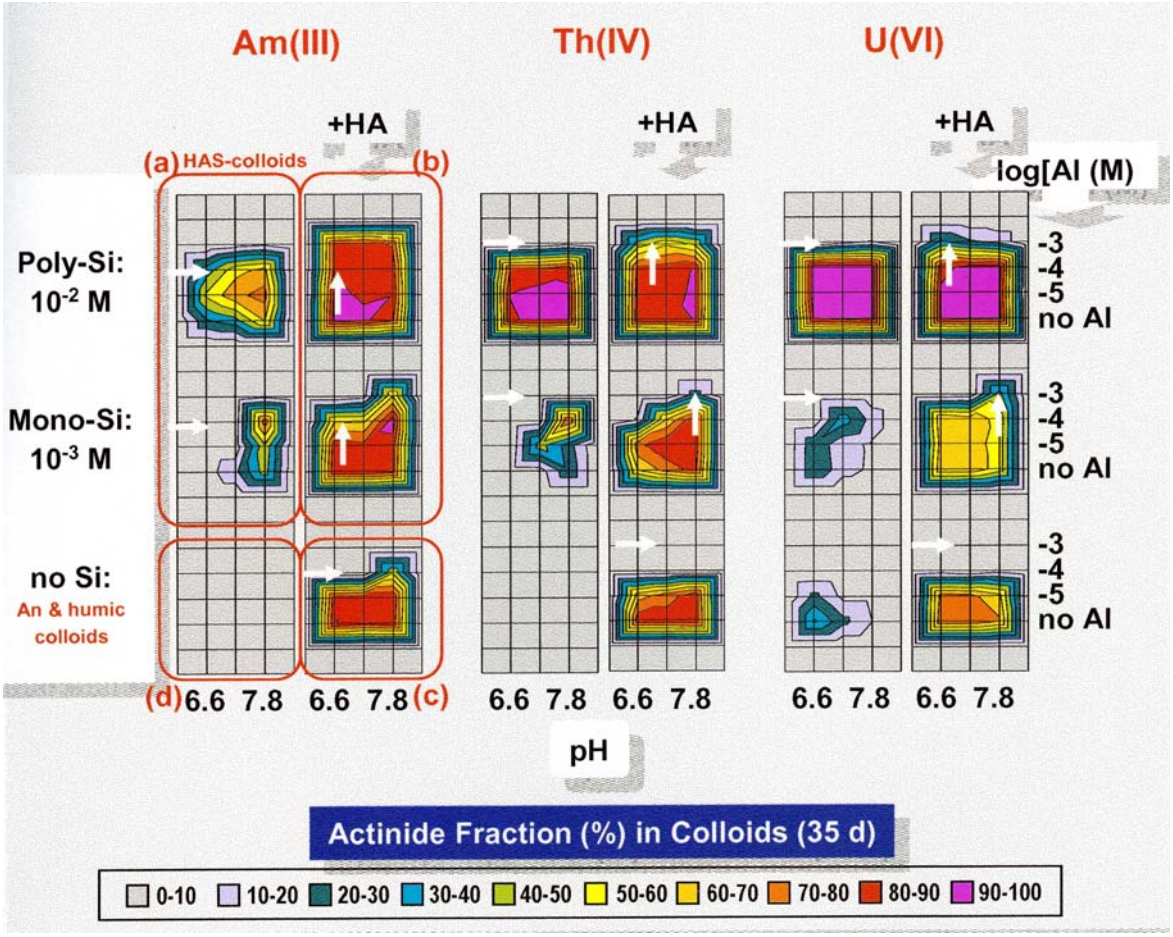

Figure 21 Actinide activity fraction (%) in the colloidal phase as a function of pH after 35 days sample conditioning time, for the following samples: HAS-colloids generated from polysilicic and mononosilicic acid (left part of the graphs-top and middle contours); HAS-humic colloids (right part of the graphs-top and middle contours); humic colloids (right part of the graph-the contours at the bottom), in solutions containing only the An (left part-the contours at the bottom). Actinide concentration in the samples is $5x10^{-8}$ M Am / $5x10^{-8}$ M Th / $8x10^{-7}$ M U. HA concentration is 6.5 mg/l.

In HAS solutions formed from monosilicic acid the actinde fraction in the colloids is generally poor, except for Am and Th at pH 7.8. In presence of humic acid, as illustrated by the contours on the right side of the diagram, one can observe an enhanced activity fraction in the colloidal phase. As previously discussed for Am, addition of HA converts the precipitated An-HAS to colloids. The formation of colloid-borne actinides becomes

promoted for the entire pH range and Al concentration range. In presence of humic colloids and Al but without silicic acid (the contours at the bottom of the right side diagram), formation of colloid-borne actinides is favoured except for Al concentrations exceeding the proton exchange capacity of HA. These conditions occur for 10^{-4} -10^{-3} M Al, for which the An/Al-humate complexes precipitate. With the addition of silicic acid we observe a change of the incorporation patterns (from the lowest part contours to those at the top and middle part of the diagram). Hence, formation of colloid-borne actinides is enhanced under all conditions mentioned above causing initial precipitation of actinides. Only in the case of U, the presence of both HAS-monosilicic acid (10^{-3} M Si/ 10^{-5} M Al) and humic colloids appears to be less favourable for colloids formation as compared to the reaction with humate colloids. In absence of HAS, U complexation with humic colloids is favourable at these HA and Al concentration. The presence of monosilicic acid, which does not favour formation of colloid-borne U, leads to a decrease of the fraction of colloid-borne U. However, as in the case of Am, the results for Th and U show that the simultaneous presence of both HAS and HA enhances generally the actinide colloid fractions.

The behaviour of the actinides is further analyzed under particular conditions indicated in Figure 21 by arrows, where the formation of colloid-borne actinides depends sensitively on the individual components under consideration, Si, Al and HA. The experimental conditions are chosen so that the competing effect of silicic and humic acid can be better evidenced. The results are depicted in Figure 22, 23 and 24.

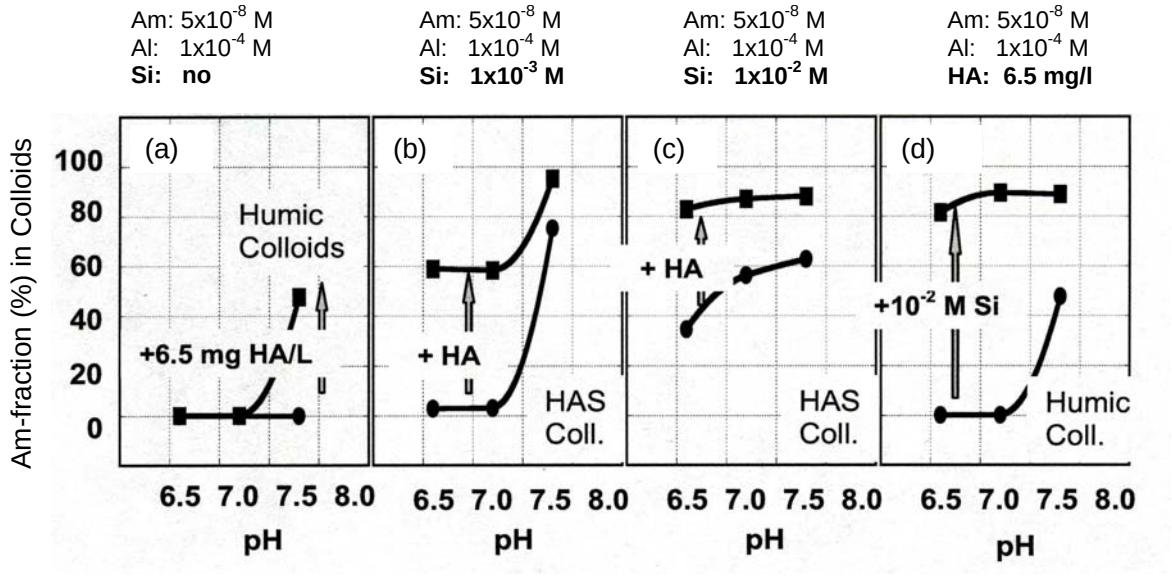

Figure 22 Formation of colloid-borne Am as a function of pH after 35 d conditioning time for the following samples: a) Al (Am) + HA, b) Al (Am) + monosilicic acid + HA, c) Al (Am) + polysilicic acid + HA, d)

Al(Am) + HA + polysilicic acid. Initial samples composition is indicated above each graph. HA or Si is added after 1 h conditioning time of the mother solution.

Figure 22 illustrates formation of colloid-borne Am under different conditions. In blank Al(Am) solution (Figure 22a) Am is precipitated in the given pH range and no colloid formation is observed. Addition of HA results in the formation of a marginal fraction of humic colloid-borne Am only at pH 7.8. The result can be expected, because the formation of Am/Al-humate colloids at Al concentration of $1x10^{-4}$ M requires HA concentration of at least 10 mg/l HA at pH 6.6 (Figure 7) and more than 3 mg/l at pH 7.8. Accordingly, the offered amount of humic acid available in the present experiment is, depending on pH, below and above the required one. The HAS-colloid generation can be observed in Figure 22b by addition of 10^{-3} M monosilicic acid, only at pH 7.8. The colloid formation is then enhanced by addition of HA following the conversion of the precipitate to colloids. Upon increasing Si concentration to 10^{-2} M (Figure 22c) in which polysilicic acid prevails, the formation of HAS-colloid-borne Am becomes significant even at lower pH. At the same time, humic acid further enhances the colloid formation under identical conditions. Figure 22d depicts the results obtained for samples with the same final composition as in Figure 22c, but prepared in different sequence of component addition, i.e. 10^{-2} M Si is added to the Al/Am-humate. As can be seen, both experiments lead to the same final results, indicating that different order of component addition does not affect the formation of colloid-borne Am and the equilibrium is reached.

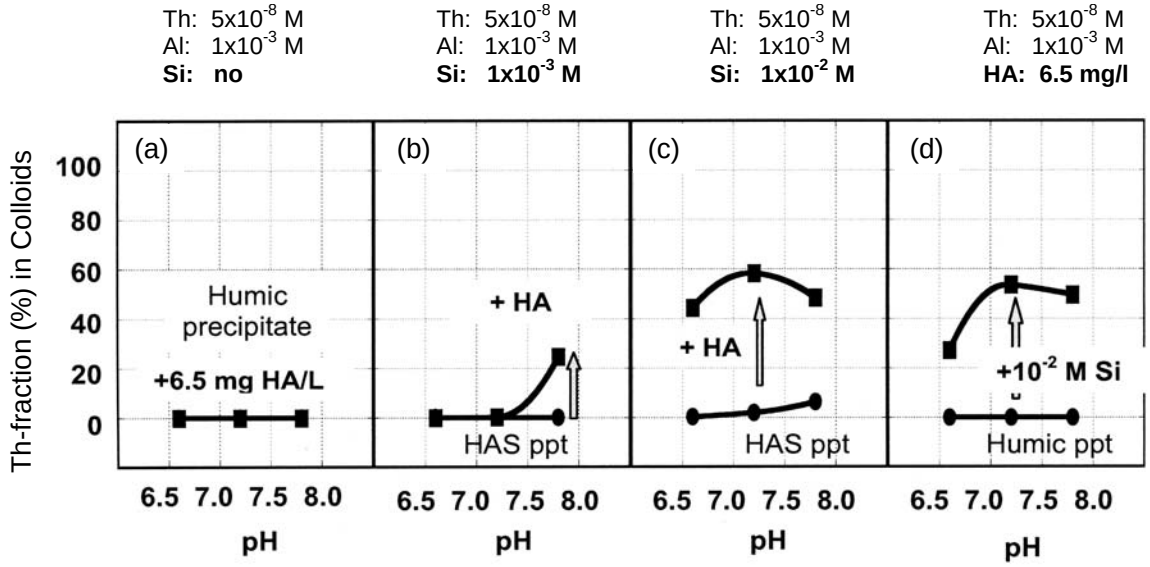

Figure 23 Formation of colloid-borne Th as a function of pH after 35 d conditioning time for the following samples: a) Al (Th) + HA, b) Al (Th) + monosilicic acid + HA, c) Al (Th) + polysilicic acid + HA, d) Al(Th) + HA + polysilicic acid. Initial samples composition is indicated above each graph. HA or Si is added after 1 h conditioning time of the mother solution.

Figure 23 and 24 illustrate the behaviour of Th and U in mixed HAS/HA solutions. In the blank samples containing Al/Th (U) (Figure 22a and 24a) the actinides are in the precipitate phase and after addition of HA the actinides remain as humate precipitate. The offered HA concentration of 6.5 mg/l is much below the required one for the formation of Al/Th(U)-humate colloids at the present Al concentration. In HAS solutions prepared out of monosilicic acid (Figure 23b and 24b) Th(U)-HAS are precipitated. After addition of HA, the conversion of the precipitate to colloid-borne actinide species can be observed for both Th and U at pH 7.8. In HAS solutions prepared from polysilicic acid (Figure 23c and 24c), minor fractions of colloids form only at pH 7.8. HA addition enhances significantly the fraction of colloid-borne Th in the entire pH range. In the case of U, the HA effect is pronounced only at pH 6.6. The results indicate the synergic action of HAS and HA at binding the actinide.

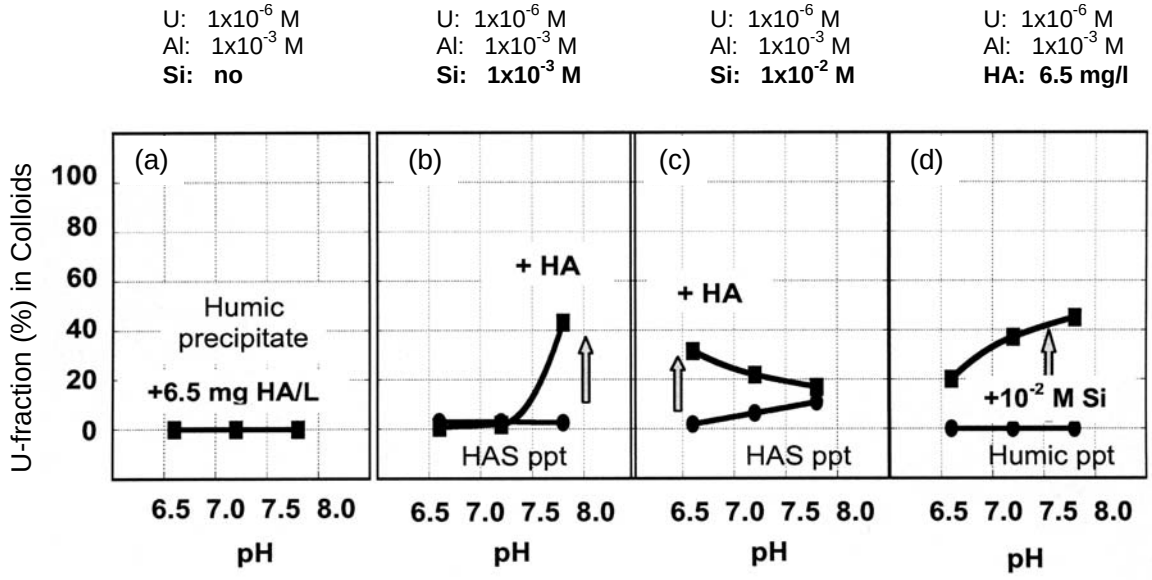

Figure 24 Formation of colloid-borne U as a function of pH after 35 d conditioning time for the following samples: a) Al (U) + HA, b) Al (U) + monosilicic acid + HA, c) Al (U) + polysilicic acid + HA, d) Al(U) + HA + polysilicic acid. Initial samples composition is indicated above each graph. HA or Si is added after 1 h conditioning time of the mother solution.

Figure 23d (24d) illustrates the results obtained for the experimental solutions having the same final composition as those described in Figure 23c (24c) but prepared by reverse sequence of reactant addition. The initial precipitated Al/Th(U)-humate are partially converted to colloids by addition of polysilcic acid. At this point a different behaviour of Th and U can be distinguished. In the case of Th, as can be seen from the upper graphs of the Figure 23c and 23d, the increase of the colloid-borne Th fraction appears to be

generally the same irrespective of the sequence of reactant addition. In contrast, in the case of U, the order of reactant addition appears to affect the formation of colloids at pH 7.2 and 7.8. Under these conditions, the fraction of colloid-borne U is larger at addition of polysilicic acid to the humic precipitate. This indicates that for U the equilibrium of the colloid formation is not attained within the 35 d observation time. The reason might be a slow kinetics associated to the conversion of the precipitate to the colloids.

Spectroscopic speciation of colloid-borne Cm(III)

For obtaining a further insight into the possible synergic effect for formation of HAS-An-humic colloids, TRLFS is applied [34] further. As for the previous investigations based on TRLFS [1], the optically sensitive Cm is chosen as a chemical analogue of Am. Speciation is conducted measuring the fluorescence emission by exciting at two different wavelengths: 370 nm and 383 nm. At the excitation wavelength of 370 nm, the light absorption of Cm is minimal and mainly the humic acid absorbs. On the other hand at the excitation wavelength of 383 nm, the light is absorbed primarily by Cm and to a less extent by humic acid. Speciation is carried out for three different colloid samples prepared as in the case of the radiometric experiment but in presence of $5x10^{-8}$ M Cm: Cm + HAS and Cm + HA as reference samples, and a sample containing Cm + HAS +HA. The speciation results are illustrated in Figure 25.

As can be seen in Figure 25a, for the reference sample Cm+HA, the Cm species excited at the two different excitation wavelengths generates two consistent emission peaks at 602.7 nm with comparable intensities at ratio I(383)/I(370) of 0.92. This ratio indicates that an indirect excitation via humic acid results in a slightly higher fluorescence emission. The emission peak at 602.7 nm corresponds to the ternary humate complex of Cm(OH)HA, as confirmed in the previous study [30].

The HAS-colloid-borne Cm species shown in Figure 25b reveals emission bands with identical peak positions at 606.9 nm but distinctively different emission intensities: for direct excitation at 383 nm and indirect excitation at 370 nm. The clear difference in the heights of the two emission bands from direct and indirect excitations and the emission peak position at 606.9, together with the considerably long emission lifetime of 518 ± 25 µs imply the incorporation of Cm into the HAS colloids. These spectroscopic characteristics agree with those observed in the previous study [21].

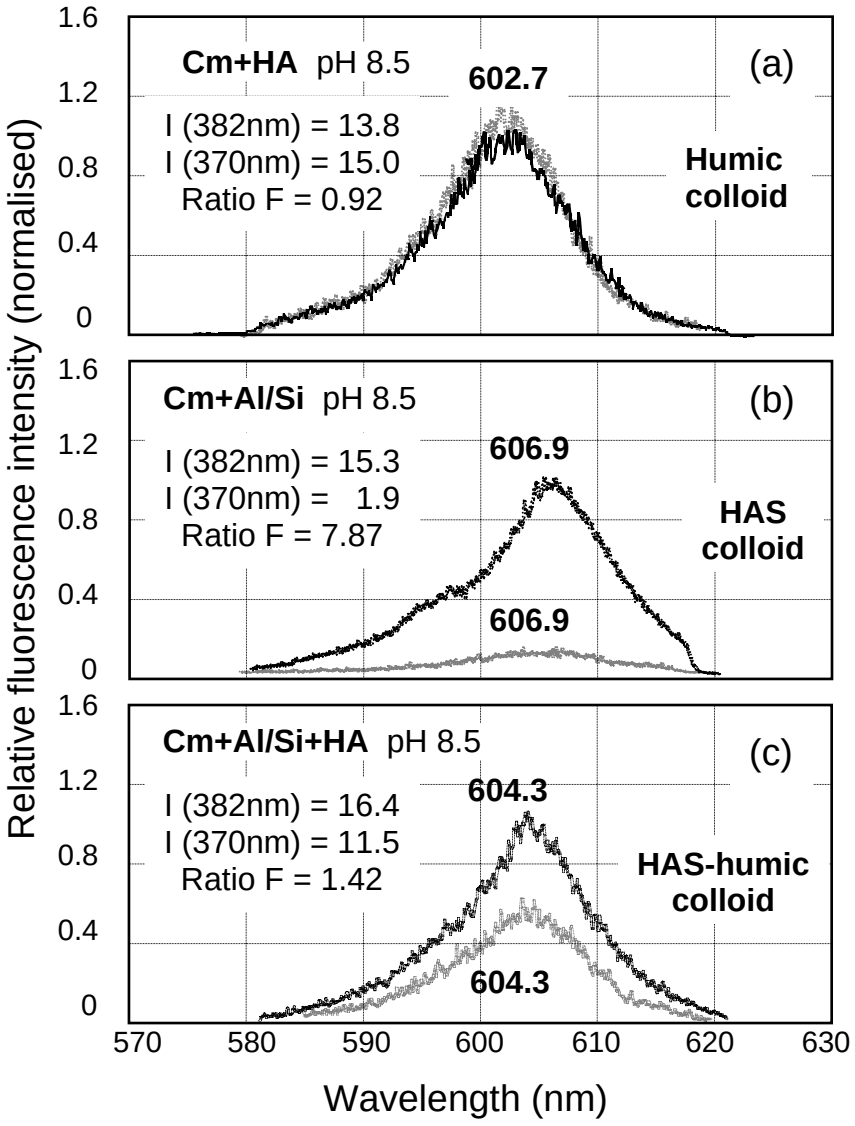

Figure 25 TRLFS speciation of Cm(III) in different solutions. Figures a-c show the fluorescence emission by direct (black) and indirect (grey) excitation of Cm in the following samples: a) humatecolloid-borne Cm in a sample containing 10^{-4} M Al and 10 mg/l HA, b): HAS colloid-borne Cm in a sample containing 10^{-4} M Al and 10^{-2} M Si, c): HAS-humate colloid-borne Cm in a sample containing 10^{-4} M Al, 10^{-2} M Si and 10 mg/l HA. Samples are prepared at pH 8.5 with 4.9 x10^{-8} M Cm.

The chemical state of HAS-colloid-borne Cm is different in presence of humic acid, as shown in Figure 25c. The emission peak position shifts to 604.3 nm, which is different from those corresponding to humic-colloid-borne Cm (602.7 nm) and HAS – colloid-borne Cm (606.9 nm). The emission intensity from indirect excitation is 70 % of the value corresponding to direct excitation. The life time of the emission, although not shown here, has been also found to change: from 518 ± 25 μs for the HAS-colloid-borne Cm (606.9 nm) to 329 ± 15 μs in presence of humic acid (604.3 nm). The life time value observed in

the mixed colloid sample is however longer than that corresponding to the humate-colloid-borne Cm of 106 μs [35]. Moreover, the position of the emission peak does not change by increasing the delay times during the lifetime measurements. If a mixture of the two species, i.e. the humate-borne Cm and the HAS-borne Cm would be present in the solution, then the short lived humate-borne Cm would be no longer detected during the measurements at longer delay time and one would observe an emission peak at higher wavelength characteristic to the HAS-borne Cm. The fact that this is not observed in the composite sample together with the previously mentioned characteristics regarding the emission intensity, peak position and fluorescence life time, prove that Cm, initially incorporated in the HAS-colloids undergoes partially chemical bonding to humic acid, hence forming a composite structure of the HAS-humic colloid-borne species.

The kinetics of the formation of colloid-borne Cm is examined during the TRLFS measurements. In Figure 26, the graph in the lower part depicts the results for the colloid-borne Cm species formed in the solution obtained by mixing all reactants at the same time [35]. In this case, the spectra obtained immediately after the sample preparation correspond to those already discussed and indicate the formation of a mixed humic-HAS-colloid-borne species. It is evident that the position of the emission peaks obtained at direct and indirect excitation of Cm, and their intensity ratio does not change significantly within 20 d observation time. This fact suggests that the species equilibrium is rapidly attained in this case, as Cm has similar binding affinity for both ligands, HAS and HA, which are added simultaneously in solution.

The graph in the upper part of Figure 26 shows the results obtained at direct and indirect excitation of Cm in the mixed colloid sample generated by addition of HA to the preformed HAS-colloid-borne Cm, which is the order of reactant addition corresponding to the radiometric experiment discussed above. Immediately after the sample preparation, as can be seen in Figure 26 (upper left panel), the colloid-borne Cm species present in the solutions show two distinct emission peaks at 605.5 and 606.9 nm and with different intensities at a ratio of 4.27. Since the most intense peak at 606.9 obtained at direct excitation corresponds to the HAS-Cm, as outlined above, the results suggest that the HAS-Cm species dominates in the solution immediately after preparation of sample. After 20 d conditioning time of the mother solution, the spectrum reveals the emission peak at approximately 604 nm corresponding to the mixed HAS-humate-colloid-borne Cm. Also, the intensity of the emission corresponding to indirect excitation of Cm increases leading to a peaks intensity ratio of 1.66.

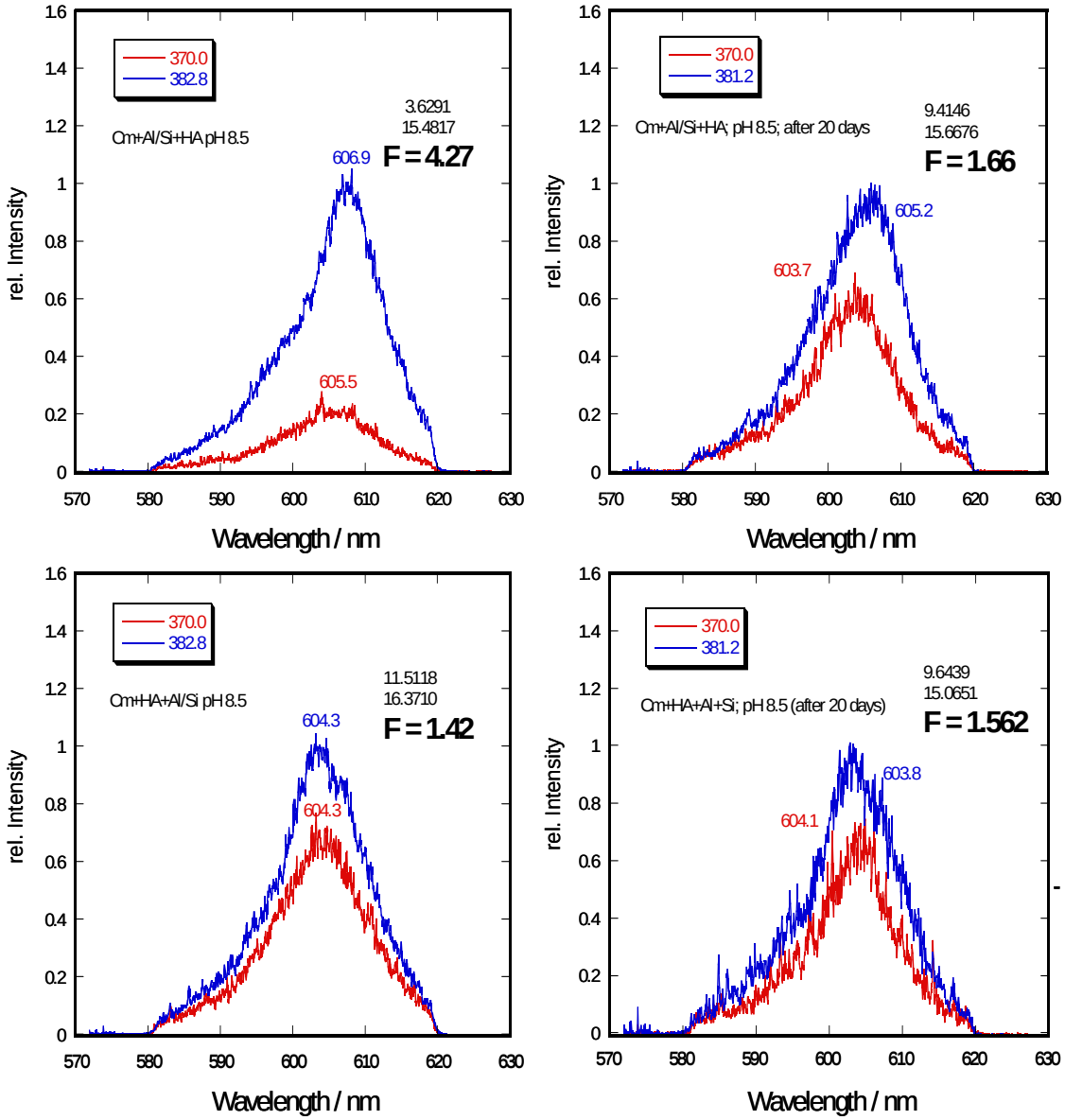

Figure 26 Florescence emission spectra of Cm (4.9×10^{-8} M) at direct (blue) and indirect excitation (red) immediately (left) and after 20 d (right) sample conditioning time. Upper part of figure: samples prepared by addition of HA to a Cm-HAS solution; Lower part: all reactants (Cm, Al, Si, HA) are added at the same time; F= intensity ratio [35].

The results indicate the progressive complexation of Cm with HA and the formation of a prevailing mixed humic-HAS species. Thus, the kinetic effect appears to be associated with the equilibration time necessary for the process of HAS partial displacement by HA from the already formed HAS-Am, followed by the formation of the mixed colloid species. The results of the fluorescence lifetime measurements (not shown here) also indicate a similar trend [35]. Hence, immediately after sample preparation different life times are measured depending on the order of reactant addition, whereas after 20 d conditioning the

values are quite close, irrespective of the order of reactant addition, indicating the equilibrium to be reached.

3.6 Stability and average particle size of HAS - humic colloids

The mixed HAS-humic colloids under discussion are analyzed by the laser-induced breakdown detection (LIBD) method [34] for monitoring their average size and number density as a function of time. To facilitate experimental handling of LIBD, Cm is replaced by its chemical homologue Eu. HAS-humic colloids are generated with or without addition of Eu ($1x10^{-7}$ M) in a solution containing $1x10^{-4}$ M Al, $1x10^{-2}$ M Si and 8 mg/l HA at pH 8.5, following the conditions applied for generating composite colloids as proved by TRLFS. For up to 58 days the monitored results are shown in Figure 27.

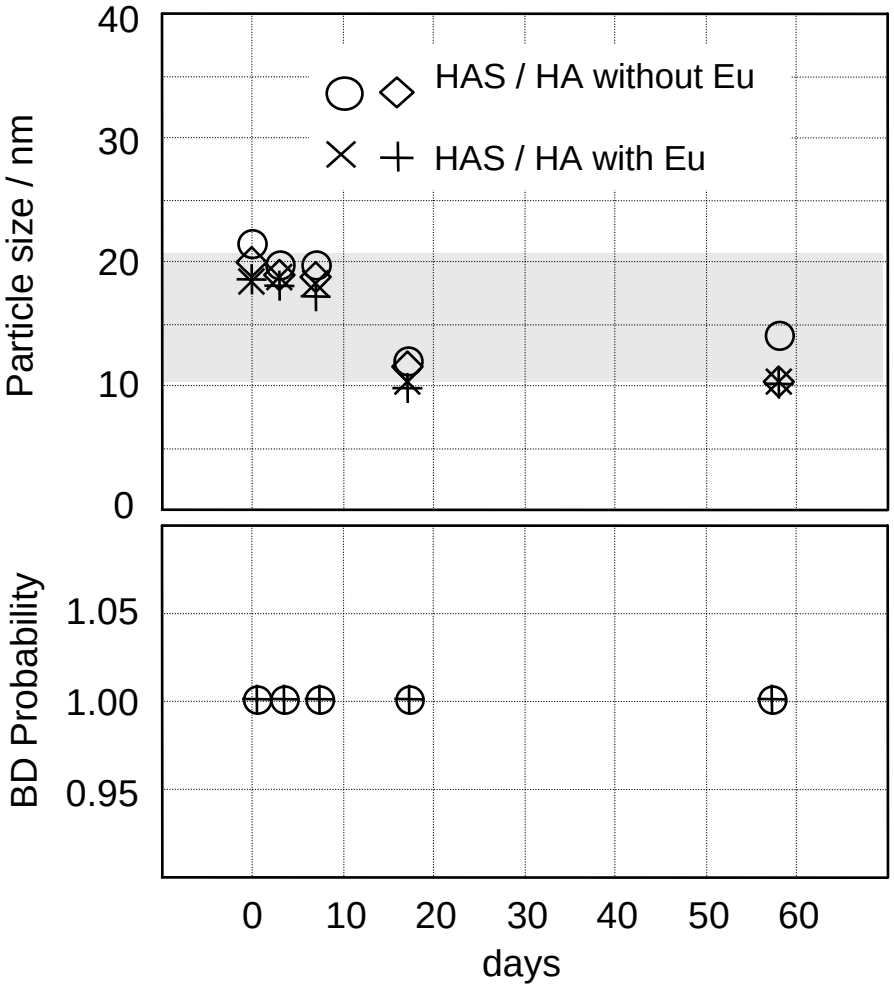

Figure 27 Particle size and breakdown (BD) probability of HAS – humic colloids determined by LIBD as a function of time fort he samples ($1x10^{-4}$ M Al, $1x10^{-2}$ M Si and 8 mg/l humic acid without and with Eu ($1x10^{-7}$ M) at pH 8.5 [34].

The average size of the predominant colloids is found to be of approximately 20 nm immediately after generation, either with or without Eu. After 10 days colloids become dispersed somewhat as the average size decreased slightly to about 10 nm which remains nearly constant up to 58 days. The number density observed by the breakdown probability is found from the beginning at a saturation state of the LIBD sensitivity, because of the a high amount of colloids generated under the given experimental conditions. The saturation state remained unchanged with time which suggests that no colloid precipitation takes place.

The results shown in Figure 27 explain the stability of HAS-humic colloids. According to these results, trivalent actinides incorporated into colloids of such compostition are expected to remain stable in an aquifer system.

4 Conclusions

The formation and stability of the HAS-colloid-borne actinides has a maximum at neutral and slightly alkaline pH in the presence of polysilicic acid. Under these conditions, the tendency for the co-nucleation with the HAS is higher for the more hydrolyzed actinides ions. On the other hand quite stable HAS colloids might exist in water solutions at the naturally relevant concentration of silicon and aluminium at circum - neutral pH. A marginal amount of actinides might be associated with those colloids over long time periods.

The formation of humate-colloid-borne actinide species is very efficient for trace amounts of actinides species at the average concentration level of HA encountered in natural waters and in the circum-neutral pH range. In contrast to the case of HAS colloids, the generation of humate-colloid-borne actinide species is distinctively favored for the nonhydrolyzed ionic species.

The simultaneous presence of HA and HAS is found to enlarge the region of colloids stability. The observed fact can be ascribed to different and complementary mechanisms of HAS and HA for binding actinide ions. The type of the colloid-borne actinide species which forms is determined by the actinide hydrolysis behaviour. Accordingly, actinides can be incorporated into HAS colloids of aluminosilicate composition via co-nucleation of hydrolyzed species (Al, actinide, and Si) or bound to humic colloids made of humic acid via complexation with the ionic metal species. Eventually, partially-hydrolyzed metal (actinide) ion species can be simultaneously bound to HAS-humic colloids through synergic bond coupling with humic molecules and HAS colloids. Nevertheless, the equilibrium between the non-hydrolyzed ionic and hydrolyzed actinide species, determining which kind of colloid-borne species forms, is finally governed by the specific conditions, i.e. the oxidation state of the actinide and its concentration together with the environmental characteristics (e.g. pH). The synergic colloid effect is mostly pronounced if the conditions of pH, concentration of Al, actinide, and humic acid are such, that Al is fully hydrolyzed, whereas the actinide becomes partially hydrolyzed, thus conucleating with Si and Al (HAS colloids) on the one side and complexing with humic colloids on the other side.

Since in natural waters HAS and humic colloids are always present to some extent as representatives for inorganic and organic colloids, in natural aquatic systems the actinides will play an important role as colloid-borne species, with high potential for migration in

the geosphere. From the present study can be concluded that the overall stability of real HAS and/or HS – metal species in natural waters is an intricate function of both thermodynamic and kinetic factors superimposed by transformation processes proceeding over a long period of time. Apart from trying to approach the complex natural conditions, the study provides a better understanding of the underlying mechanisms of aquatic actinide colloids formation.

5 Appendix A

Spectrophotometric Determination of Al in Presence of EDTA and Soluble Silicates by Complexation with Chromazurol S.

Abstract

The Merck standard procedure (Spectroquant® 1.14825 - determination of Al through its complexation by Chromazurol S in an acetate-buffered solution) is adopted to measure Al in presence of a 10-fold excess of EDTA. Pb(II) forms a more stable complex with EDTA and it is used as an EDTA-masking agent. The exchange reaction of the Al-EDTA complex with Pb is complete in acidic medium within 1 h at room temperature. Al(III) determination is possible in the linear range of 7×10^{-6} up to 1×10^{-4} mol/l, with a detection limit of 3×10^{-6} mol/l or 0.08 mg/l.

Introduction

It is well known that elevated Al concentrations in natural water are toxic to aquatic and terrestrial organisms. EDTA is present in many aquatic systems resulting from its role as a synthetic chelating agent used in many industrial applications and due to its low biodegradability. Therefore, the development of methods for the determination of the Al content in the presence of EDTA can be useful. Many methods have already been developed for the determination of Al. These days, these methods include ICP-MS, ICP-OES, AAS, NMR and etc. However, because these instrumental analyses require rather expensive equipment and higher running costs, they offer limited availability. Spectrophotometry is a relatively easy alternative method, which has been applied to the determination of Al. Chromazurol S in an acetate-buffered solution is one of the most widely used chromogenic reagents for Al complexation (Spectroquant® 1.14825 Merck standard procedure). However, the Al ions cannot be determined without decomposition of the Al-EDTA complexes. There is the method for photometric determination subsequent to

microwave-assisted decomposition with Oxisolv® (Spectroquant® Crack Set 10). The decomposition with Oxisolv® in the microwave digestion unit destroys the metal complex and allows the determination of the metal content. Nevertheless, we use Pb(II) ions in excess concentration to destroy the Al-EDTA complex.

Experimental

Equipment

- Automatic titrator 736 Gp Titrino, Tinet 2.4 software, Metrohm
- Balance, Mettler AT 250 - 0.00001 g sensitivity
- Centrifuge Biofuge primo Heraeus-Kendro
- Magnetic stirrer
- pH-meter Metrohm AG 8.713.1001
- Pipette tips 10 µl, 100 µl, 200 µl, 1000 µl, 5000 µl
- Pipettes 2.5 µl, 10 µl, 20 µl, 200 µl, 1000 µl Eppendorf
- Plastic disposable pipettes 1 ml, 5 ml, 10 ml
- Polyethylene vials 1000 PCS MAXI VIAL^{tm} 18 ml, Packard Bioscience, 6000203
- Quartz cuvettes
- Spectrophotometer Carry 5000, Cary WinUV 3.0 (4000/5000/6000i) Software
- Sterile filters Millex 0.45 µm Millipore Corporation
- Syringes 5 ml
- Ultrafiltration cells, 2 ml, 5 ml Amicon
- Ultrafiltration membranes Centricon YM-10, 10000 MW cut-off, Millipore Corporation

Reagents

- Silicon ICP/DCP standard solution contains 10000 µg/ml of Si in 3 wt.% NaOH;
- Aluminium ICP/DCP standard solution contains 10050 µg/ml of Al in 1-4 wt.% HCl;
- Hydrochloric acid 30% Suprapur®;
- Sodium hydroxide solution 30% Suprapur®;
- Ethylendiaminetetraacetic acid tetraacetic, disodium salt, EDTA

All chemicals are used without further purification. Working solutions are prepared daily by diluting the stock solutions. 1 M EDTA stock solution is prepared from its disodium salt

in Milli-Q water. All experiments are open to the atmosphere and are conducted at ambient temperature.

Results and Discussion

The absorption spectra of Al(III) either in the presence or absence of silica and EDTA are graphically presented in Figure 28. The absorbance spectrum, expressed as the difference of the blue-red coloration of the sample solution against the brownish-yellow blank, exhibits a maximum at 548 nm. The absorbance curves do not show a maximum at 548 nm in presence of EDTA. Hence, the Al-EDTA complex cannot be determined without decomposition. Silica in oligomeric state also successfully competes with cromazurol S to complex Al.

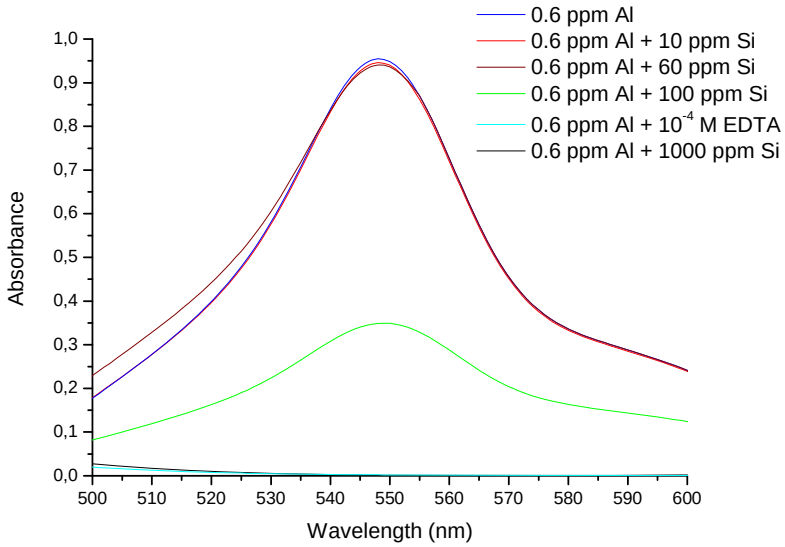

Figure 28 UV absorption spectrum of Al-cromazurol S complex at 25ºC. Effect of silica and EDTA concentrations on the absorption spectra of Al. (The test with a solution of 0.6 ppm Al shows the effect of H_4SiO_4 and EDTA with respect to the reduction or inhibition of the theoretical coloration).

Al(III) ions can be displaced from the EDTA complex by Fe(III) ions since the formation constant for Fe-EDTA is very high, but a combination of $Fe(OH)_m^{3-m}$ and $H_nSiO_4^{n-4}$ ions is found to interfere with determination of Al using photometry. We decided to destroy the Al-EDTA complex by addition of Pb ions in excess concentration. The formation constant

for the Pb-EDTA complex is higher then for Al-EDTA (Lg $K_{PbHEDTA^-}$ = 20.8; Lg $K_{AlHEDTA}$ = 19.0), so the exchange reaction is thermodynamically favourable at certain pH. NaOH and HCl are used for the study of pH effect on the exchange kinetics of Al-EDTA with Pb(II). In order to minimize the reaction time, a series of experiments is conducted using 1.5×10^{-3} M Pb, 1.2×10^{-4} M Al, and 2.5×10^{-4} M EDTA at various pH values.

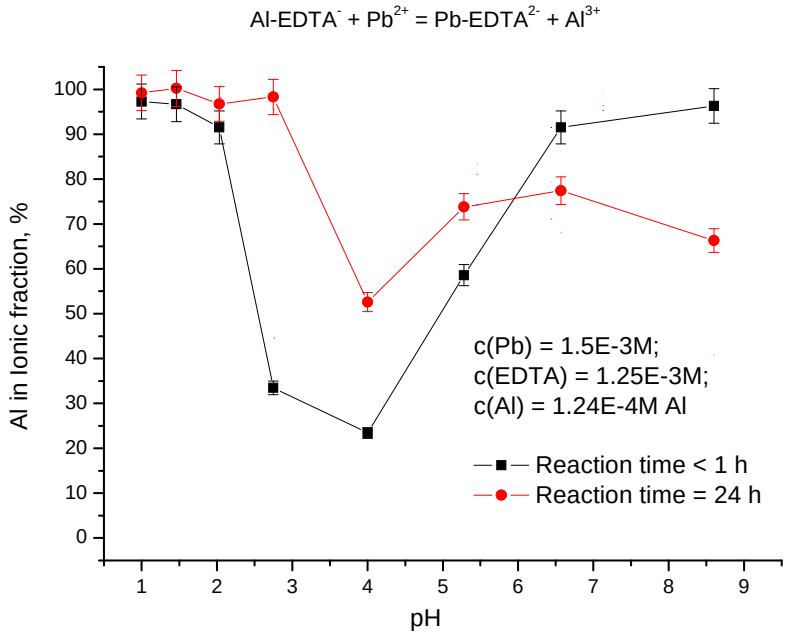

Figure 29 Effect of pH on the reaction Al-EDTA$^-$ + Pb^{2+} = Pb-EDTA^{2-} + Al^{3+}.

As can be seen from Figure 29, the exchange reaction of the Al-EDTA complex occurs at slow rates at ambient temperature and pH = 4 even with a large excess of the Pb concentration. The reaction is relatively fast at pH 1 and completes within 1 hour at room temperature. Consequently, a 0.1 mol/l HCl solution is adopted for further experiments. The effect of Pb concentration on the height of the absorption peak is tested over the range of 1.25×10^{-4} to 9×10^{-3} mol/l. The peak height increases with increasing the Pb concentration and becomes constant at a concentration range from 0.3 mmol/l up to 5 mmol/l. Although the height of the peak gradually increases at Pb concentrations more than 5×10^{-3} mol/l, the difference abs548 – (abs593 + abs503)/2 remains constant up to 1×10^{-4} mol/l, as can be appreciated from Figure 30.

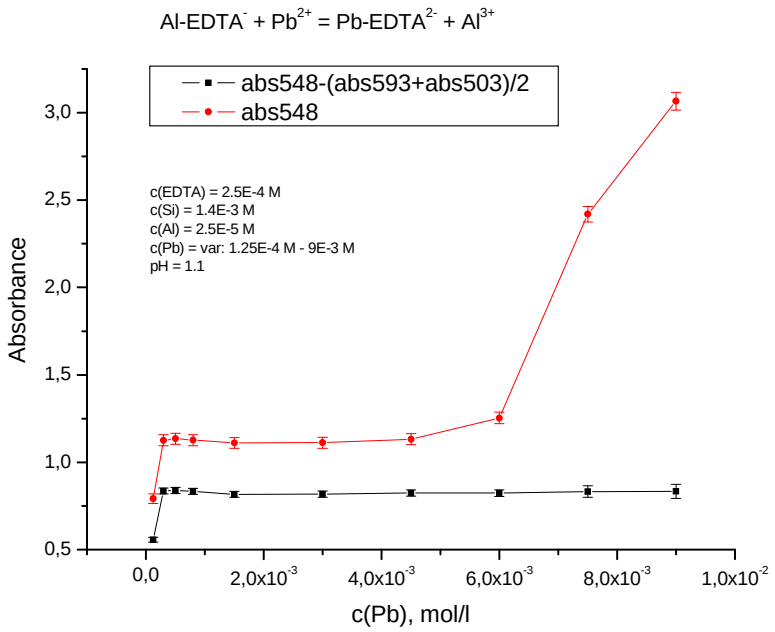

Figure 30 The effect of Pb concentration on the height of the absorption peak.

The addition of up to 20-fold Pb(II) excess over EDTA concentration does not affect the absorbance of the Al-Chromazurol complex at 548 nm, so Pb (II) ions are used further as an EDTA-masking agent. Therefore, an optimum range of Pb concentrations, namely $1\times 10^{-3} \div 4 \times 10^{-3}$ mol/l, is used for the following work.

Procedure

Calibration curve, limit of detection and precision.

A series of solutions containing 1.8×10^{-3} mol/l Si, 1.3×10^{-3} mol/l EDTA and a defined amount of Al(III) ions ($1.5\times10^{-6} \div 9\times10^{-5}$ mol/l) is prepared. To those solutions, 10 µl 1.5 M $Pb(NO_3)_2$ is added to give a final concentration of 3×10^{-3} mol/l Pb. The solutions are mixed thoroughly and then 25 µl of 9 M HCl is added to give a pH of about 1. The contents are again mixed well and are diluted to 5 ml with Milli-Q water. The solutions are then left to equilibrate for 1 h at room temperature, then the Al-test is performed following the Merck standard procedure (Spectroquant® 1.14825). 23 µl of 10 M NaOH is added to each sample to decrease acidity before adding the reagents. After mixing the solutions, aliquots of each solution are pipetted into 10 mm quartz cuvettes. The calibration curve is prepared by plotting the concentration (mol/l) of Al(III) against the absorbance at 548 nm.

A linear relationship is obtained over the concentration range 7×10^{-6} to 1×10^{-4} mol/l of Al(III) corresponding to 0.19 to 2.7 mg/l.

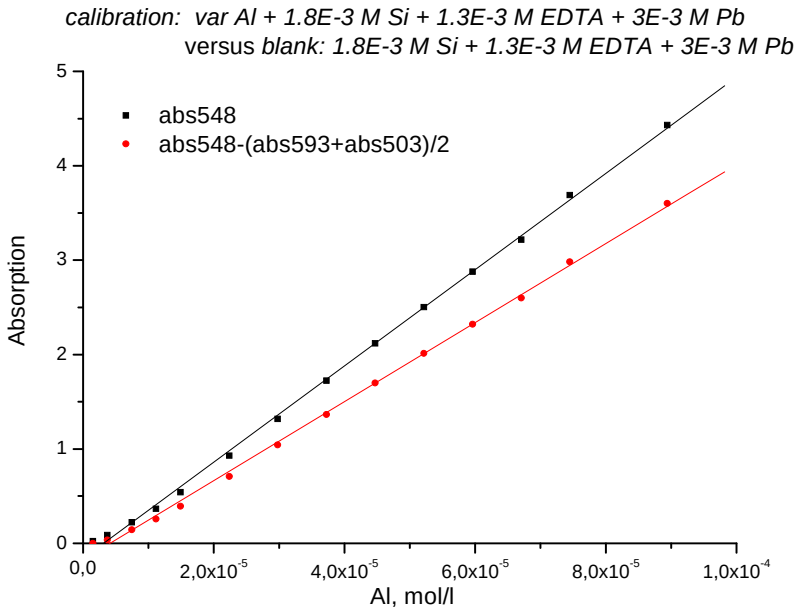

Figure 31 Calibration curve.

The proposed method is validated using ICP-OES analysis. As can be seen from Table 11, the corresponding results are in good agreement with those from ICP-OES analysis.

Table 11 Determination of Al by spectrophotometric and ICP-OES analysis.

N	Chemical composition of synthetic mixture	Method of determination	
		Carry 5000	ICP-OES (Vista Pro Varian)
1	1.3×10^{-3} M EDTA, 1.8×10^{-3} M Si, Al	$5.77(18)\times10^{-5}$ M	$5.84(6)\times10^{-5}$ M
2	1.3×10^{-3} M EDTA, 1.8×10^{-3} M Si, Al	$2.51(8)\times10^{-5}$ M	$2.63(3)\times10^{-5}$ M
3	1.3×10^{-3} M EDTA, 1.8×10^{-3} M Si, Al	$2.84(8)\times10^{-5}$ M	$3.01(3)\times10^{-5}$ M
4	4.3×10^{-4} M EDTA, 2.1×10^{-3} M Si, Al	$2.49(8)\times10^{-5}$ M	$2.57(3)\times10^{-5}$ M

The reproducibility of the method is obtained by analyzing 12 replicates containing 1.2×10^{-4} M of Al(III). Two solutions containing 1.4×10^{-3} mol/l Si, 1.3×10^{-3} mol/l EDTA and 1.2×10^{-4} M Al(III) are prepared in the following way: Al is pre-equilibrated with

EDTA at pH 2 for 3 hours and then monomeric Si is introduced using an automatic titrator, 2 to 4 ml aliquots are taken. Each aliquot is prefiltered through 450 nm syringe filters and then is filtered further through a membrane filter with a nominal molecular-weight cut-off of 10 kDa. Al passing through the second filter is defined as dissolved. Dissolved Al is analyzed by a spectrophotometer using the Al-Chromazurol complex.

Table 12 The reproducibility of spectrophotometric analysis.

N	Aliquot, ml	Absorption at 548 nm	$C(Al_{ionic\ fraction})$, M
1	3.17	3.842	1.23E-04
2	3.61	4.143	1.16E-04
3	3.43	3.997	1.18E-04
4	2.23	2.646	1.24E-04
5	3.32	3.947	1.21E-04
6	2.14	2.509	1.23E-04
7	2.97	3.583	1.23E-04
8	3.51	4.075	1.18E-04
9	3.33	3.921	1.19E-04
10	2.56	3.074	1.24E-04
11	3.18	3.823	1.22E-04
12	2.2	2.602	1.23E-04

As can be appreciated from Table 12, the relative standard deviation of the determined aluminum concentration is 2 %.

Using the Cary 5000 Fluorescence Accessory, an analytical procedure for the direct fluorimetric trace determination of Al(III) ions has been developed, with a detection limit of 3×10^{-6} mol/l or 0.08 mg/l. The proposed method is simple and relatively rapid. The method is potentially useful for the analysis of Al(III) in factory effluents containing EDTA.

6 Appendix B

Nomenclature

AFM	Atomic Force Microscopy
An	Actinide
Da	Dalton
EDTA	Ethylenediamine tetraacetic acid
EDX	Energy dispersive X-ray
g	gravitational acceleration
HA	Humic acid
HAS	Hydroxyaluminosilicate
HS	Humic substances
ICP-OES	Inductively Coupled Plasma - Optical Emission Spectroscopy
IEP	Isoelectric point
IIIF	Institut für Interdisziplinäre Isotopen Forschung
INE	Institut für Nukleare Entsorgung
LC	Loading capacity
LIBD	Laser Induced Breakdown Detection
LSC	Liquid Scintillation Counting
MOPS	3-[N-morpholino] propanesulfonic acid
PEC	proton exchange capacity
ppm	parts per million (10^{-6}g/g)
pHpzc	pH value (-log[H+]) at zero surface charge
SEM	scanning electron microscopy
TRLFS	time resolved laser fluorescence spectroscopy
UV-VIS	Ultraviolet-Visible domain of light

7 References

[1] M. A. Kim, P. J. Panak, J. I. Yun, J. I. Kim, A. N. Priemyshev, and K. Köhler, Abschlußbericht BMWi, Bundesministerium für Wirtschaft und Industrie, RCM Report 012004, Technische Universität München, 2004.

[2] M. A. Kim, A. N. Priemyshev, D. C. Breban, P. J. Panak, J. I. Yun, and J. I. Kim, Abschlußbericht BMWi, Bundesministerium für Wirtschaft und Technologie, RCM Report 012007, Technische Universität München, 2007.

[3] J. I. Kim, Mater. Res. Soc. Symp. Proc, 1993, **294**, 3.

[4] J. M. Duan and J. Gregory, Colloids and Surfaces a-Physicochemical and Engineering Aspects, 1996, **107**, 309.

[5] C. Degueldre, I. Triay, J. I. Kim, P. Vilks, M. Laaksoharju, and N. Miekeley, Applied Geochemistry Journal, 2000, **15**, 1043.

[6] J. I. Kim, D. S. Rhee, G. Buckau, and A. Morgenstern, Radiochimica Acta, 1997, **79**, 173.

[7] J. I. Kim, P. Zeh, and B. Delakowitz, Radiochimica Acta, 1992, **58-9**, 147.

[8] J. I. Kim, MRS Bulletin, 1994, 47.

[9] J. I. Kim, Nuclear Engineering and Design, 2000, **202**, 143.

[10] J. F. McCarthy, K. R. Czerwinski, W. E. Sanford, P. M. Jardine, and J. D. Marsh, Journal of Contaminant Hydrology Journal, 1998, **30**, 49.

[11] A. B. Kersting, D. W. Efurd, D. L. Finnegan, D. J. Rokop, D. K. Smith, and J. L. Thompson, Nature, 1999, **397**, 56.

[12] M. I. Litaor, Health Physics, 1999, **76**, 171.

[13] J. I. Kim, Radiochimica Acta, 1991, **52/53**, 71.

[14] T. Rabung, T. Stumpf, H. Geckeis, R. Klenze, and J. I. Kim, Radiochimica Acta, 2000, **88**, 711.

[15] A. Mori, W. R. Alexander, H. Geckeis, W. Hauser, T. Schafer, J. Eikenberg, T. Fierz, C. Degueldre, and T. Missana, Colloids and Surfaces A: Physicochemical and Engineering Aspects, 2003, **217**, 33.

[16] J. I. Kim, B. Delakowitz, P. Zeh, D. Klotz, and D. Lazik, Radiochimica Acta, 1994, **66-7**, 165.

[17] R. Artinger, T. Rabung, J. I. Kim, S. Sachs, K. Schmeide, K. H. Heise, G. Bernhard, and H. Nitsche, Journal of Contaminant Hydrology, 2002, **58**, 1.

[18] R. K. Iler, 'The chemistry of silica. Solubility, Polymerization, Colloid and Surface Properties, and Biochemistry', ed. J. W. Sons, A Wiley-Interscience Publication, 1979.

[19] F. J. Doucet, C. Schneider, S. J. Bones, A. Kretchmer, I. Moss, P. Tekely, and C. Exley, Geochimica et Cosmochimica Acta, 2001, **65**, 2461.

[20] T. W. Swaddle, Coordination Chemistry Reviews, 2001, **219-221**, 665.

[21] M. A. Kim, P. J. Panak, J. I. Yun, A. N. Priemyshev, and J. I. Kim, Colloids and Surfaces A: Physicochemical and Engineering Aspects, 2005, **254**, 137-145.

[22] A. N. Priemyshev, Formation of colloids of Am, Th and aluminosilicates in aquatic systems. ISBN 3-89963-071-8, Ph.D. Thesis, 2004.

[23] M. N. Jones and N. D. Bryan, Advances in Colloid and Interface Science, 1998, **78**, 1.

[24] R. J. Silva and H. Nitsche, Radiochimica Acta, 1995, **70-1**, 377.

[25] H. Geckeis, T. Rabung, T. N. Manh, J. I. Kim, and H. P. Beck, Environmental Science & Technology, 2002, **36**, 2946.

[26] G. Buckau, FZKA-Report 6969, Forschungszentrum Karlsruhe, 2004.

[27] A. Mansel and H. Kupsch, Applied Radiation and Isotopes, 2007, **65**, 793.
[28] J. Rothe, M. A. Denecke, and K. Dardenne, Journal of Colloid and Interface Science, 2000, **231**, 91.
[29] P. D. Taylor, R. Jugdaohsingh, and J. J. Powell, Journal of the American Chemical Society, 1997, **119**, 8852.
[30] M. A. Kim, P. J. Panak, J. I. Yun, J. I. Kim, R. Klenze, and K. Kohler, Colloids and Surfaces A: Physicochemical and Engineering Aspects, 2003, **216**, 97.
[31] Z. Sun and J. D. Rimstidt, Environmental & Engineering Geoscience, 2002, **8**, 3.
[32] F. R. Livens, K. Morris, R. Parkman, and L. Moyes, Nuclear Energy-Journal of the British Nuclear Energy Society, 1996, **35**, 331.
[33] P. Reiller, V. Moulin, F. Casanova, and C. Dautel, Radiochimica Acta, 2003, **91**, 513.
[34] M. A. Kim, P. J. Panak, D. C. Breban, A. Priemyshev, J. I. Yun, A. Mansel, and J. I. Kim, Colloids and Surfaces A: Physicochemical and Engineering Aspects, 2007, **296**, 206.
[35] P. J. Panak, M. A. Kim, J. I. Yun, J. I. Kim, and T. Fanghänel, 10th International Conference on Chemistry and Migration Behaviour of Actinides and Fission Products in the Geosphere, Avignon, France, 18-23 September 2005, 2005.
[36] V. A. Rabinovich and Z. J. Chavin, 'The chemical brief handbook', Chemistry, 1994.

8 Publications, Reports and Conferences

Publications & Reports:

M.A. Kim, P.J. Panak, D.C. Breban, A. Priemyshev, J.I. Yun, A. Mansel, J.I. Kim: "Interaction of Actinides(III) with Aluminosilicate Colloids. Part IV. Influence of Humic Acid", Colloids and Surfaces A: Physicochem. Eng. Aspects 296 (2007) 206-215.

M.A. Kim, D.C. Breban, A. Priemyshev, A. Mansel, J.I. Kim: "Interaction of Actnides(IV) and Actinides(VI) with Aluminosilicate and Humic Colloids", Colloids and Surfaces A: Physicochem. Eng. Aspects, in preparation.

D. Breban, Ph.D. Thesis "Provenance and Characterization of Aquatic Actinide Colloids: Nucleation of Aluminosilicate Colloids with Actinides", Fakultät für Chemie, Ruprecht-Karls-Universität Heidelberg (2007).

A. Priemyshev, M.A. Kim, J.I. Kim: Binding affinity of humic colloids to actinides – and what's behind, 2nd. Annual Workshop Proceedings 6th EC FP – FUNMIG IP, Stockholm, November 2006.

P.J. Panak, M. Bouby, M.A. Kim, J.I. Yun, D. Breban, A. Priemyshev, J.I. Kim, H. Geckeis, Th. Schäfer: „Colloid formation processes ". FZKA 7249 Annual Report 2005 (2006) 19-22.

M. A. Kim, P. J. Panak, J. I. Yun, A. Priemyshev, and J. I. Kim: "Interaction of actinides with aluminosilicate colloids in statu nascendi: Part III: Colloid formation from monosilanol and polysilanol". Colloids and Surfaces A: Physicochem. Eng. Aspects 254 (2005) 137-145.

D. Breban, P.J. Panak, K. Dardenne, J. Rothe, M.A. Denecke, M.A. Kim, J.I. Kim, Th. Fanghänel: „Interaction of U(VI) with Silica and Aluminosilicate Colloids in Statu Nascendi". ANKA Annual Report 2005 (2005) 92-93.

Conferences:

GDCh-Wissenschaftsforum Chemie 2007, Ulm, 16. – 19. September 2007: A. N. Priemyshev: "Trace metal-humate interactions. Effect of aging time and metal concentration on the kinetic dissociation of Th(IV) from humic colloids".

2nd Annual Workshop of IP FUNMIG FP6 Integrated Project: Fundamental Processes of Radionuclide Migration, Stockholm, Sweden, November 21 – 23, 2006: A. Priemyshev, M.A. Kim, J.I. Kim: "Binding affinity of humic colloids to actinides – and what's behind".

2nd FUNMIG RTDC-2 Progress Meeting, Karlsruhe, Germany, July 31, 2006: A. N. Priemyshev, M. A. Kim, D.C. Breban, P. J. Panak, J. I. Yun, J. I. Kim, A. Mansel: "Interaction of actinides(III) with hydroxy-aluminosilicate colloids: influence of humic acid".

Abschlussworkshop zum Verbundprojekt: „Migration von Actiniden im System Ton, Huminstoff, Aquifer“, Mainz (2006): D.C. Breban, M.A. Kim, P.J. Panak, A. Priemyshev, A. Mansel, J.I. Yun, J.I. Kim: „Formation of Colloid-borne Actinides in Aluminosilicate-Humate Solutions“.

The 6th International Symposium on Advanced Environmental Monitoring, Heidelberg (2006): J.I. Kim, M.A. Kim, J.I. Yun, P.J. Panak: “Aquatic Colloids: Provenance, Characterisation and Significance to Environmental Monitoring”.

Workshop zum Verbundprojekt: „Migration von Actiniden im System Ton, Huminstoff, Aquifer“, Leipzig (2005): M.A. Kim, A. Priemyshev, Breban, A. Mansel, G. Buckau, J.I. Kim, P.J. Panak, J.I. Yun, Th. Fanghänel: “Humat- und Aluminosilicat-Kolloide im Wettbewerb um die Bildung von An(III) Pseudokolloiden”.

Workshop zum Verbundprojekt: „Migration von Actiniden im System Ton, Huminstoff, Aquifer“, Leipzig (2005): P.J. Panak, M.A. Kim, J.I. Yun, J.I. Kim, Th. Fanghänel: „Speziazion von Kolloidalen Cm(III)-Spezien im Ternären Cm-Humat-Aluminosilicat-System mit Zeitaufgelöster Laserfluoreszenz Spektroskopie“.

GDCh-Jahrestagung Chemie 2005, Düsseldorf, Deutschland, 11. – 14. September 2005: P.J. Panak, M.A. Kim, J.I. Jun, D. Breban, A. Priemyshev, J.I. Kim, Th. Fanghänel: “Aquatische Chemie von Actiniden in Natürlichen Kolloidalen Systemen”.

GDCh-Jahrestagung Chemie 2005, Düsseldorf, Deutschland, 11. – 14. September 2005: D. Breban, A. Priemyshev, M.A. Kim, P.J. Panak, J.I. Jun, J.I. Kim, Th. Fanghänel: “Provenance and Stability of Colloid-borne Actinides: Incorporation of Actinides(III, IV, V, VI) into Aluminosilicate Colloids”.

GDCh-Jahrestagung Chemie 2005, Düsseldorf, Deutschland, 11. – 14. September 2005: A. Priemyshev, D. Breban, M.A. Kim, P.J. Panak, A. Mansel, J.I. Kim, Th. Fanghänel: “The role of Humic Acid on the Formation of HAS (Hydroxyaluminosilicate) Colloid-borne Actinides”.

10th International Conference on Chemistry and Migration Behavior of Actinides and Fission Products in the Geosphere, MIGRATION '05, Avignon, France, September 18 – 23, 2005: D. Breban, A. Priemyshev, M.A. Kim, P.J. Panak, J.I. Jun, J.I. Kim, Th. Fanghänel: “Provenance and Stability of Colloid-borne Actinides: Incorporation of Actinides(III, IV, V, VI) into Aluminosilicate Colloids”.

10th International Conference on Chemistry and Migration Behavior of Actinides and Fission Products in the Geosphere, MIGRATION '05, Avignon, France, September 18 – 23, 2005: A. Priemyshev, D. Breban, M.A. Kim, P.J. Panak, A. Mansel, J.I. Kim, Th. Fanghänel: “The role of Humic Acid on the Formation of HAS (Hydroxyaluminosilicate) Colloid-borne Actinides”.

10th International Conference on Chemistry and Migration Behavior of Actinides and Fission Products in the Geosphere, MIGRATION '05, Avignon, France, September 18 – 23, 2005: P.J. Panak, M.A. Kim, J.I. Jun, J.I. Kim, Th. Fanghänel: “Formation of Colloid-borne An(III): Speciation of Ligand Competition in the An(III)-Al-Si-Humic acid System by Sensitized Fluorescence Spectroscopy”.

10th International Conference on Chemistry and Migration Behavior of Actinides and Fission Products in the Geosphere, MIGRATION '05, Avignon, France, September 18 – 23, 2005: J.I. Jun, M.A. Kim, P.J. Panak, J.I. Kim, Th. Fanghänel: “Formation of Actinide(IV) Colloids and Stabilization via Interaction with An(III)/Ln(III)”.

Acknowledgements

This work has been financially supported by the German Federal Ministry of Economics and Technology (BMWi) Research project under the contract number 02E10035.

A number of other people contributed to the realization of the present work. Thanks are due to Dr. Christian Marquardt and Dr. Gunnar Buckau from INE, for providing the radioactive standard solutions and the humic acid, as well as to Dr. Alexander Mansel (IIIF Leipzig) for labeling the humic acid.